LA-UR-97-1359

Title

Development of Nonfertile And Evolutionary Mixed Oxide Nuclear Fuels for Use in Existing Water Reactors

Compiled by

Stacey Eaton
Carl Beard
John Buksa
Ken Chidester

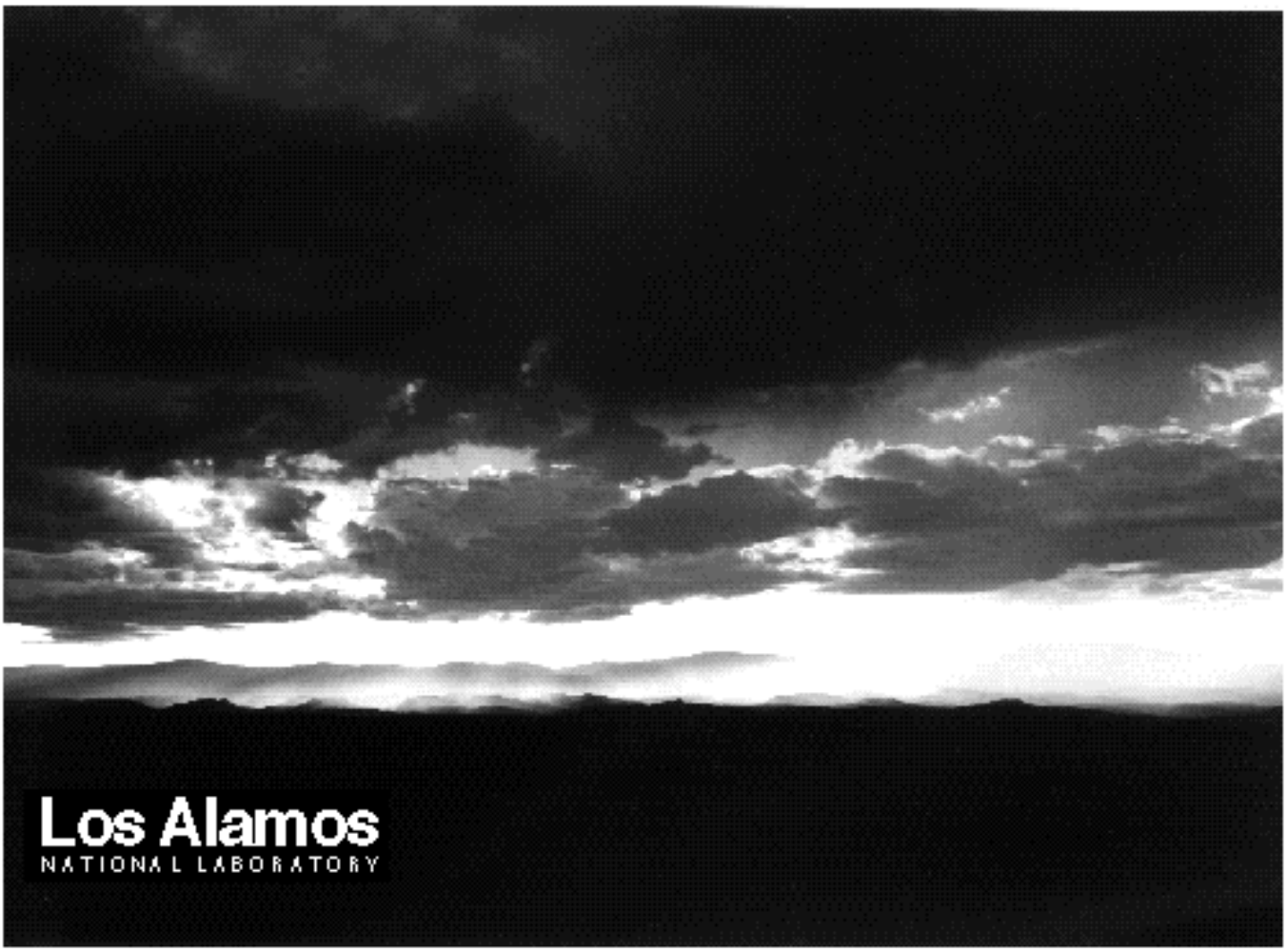

DEVELOPMENT OF NONFERTILE AND EVOLUTIONARY MIXED OXIDE NUCLEAR FUELS FOR USE IN EXISTING WATER REACTORS

Stacey Eaton, Carl Beard, Kevin Ramsey, John Buksa, and Ken Chidester
Los Alamos National Laboratory

Abstract

Investigations of an advanced fuel form are currently under way at Los Alamos National Laboratory. This new fuel form, referred to as Evolutionary Mixed Oxide (EMOX), is a slight perturbation on standard mixed oxide (MOX) fuel, and analyses show that it can be an effective plutonium management tool in existing light water reactors. The addition of a small fraction of calcia-stabilized zirconia to the uranium-plutonium oxide matrix allows for greater plutonium conversion, while also providing a licensing path towards eventual implementation of higher plutonium destruction fuels. These fuels, referred to a nonfertile (NF) fuels, achieve their high destruction rates through the absence of uranium, which breeds plutonium, in the fuel composition.

Extensive calculations have been performed to assess the feasibility of incorporating the EMOX fuel form into existing pressurized water reactor systems, and the results are detailed in this report. Specifically, calculations have been made to determine the plutonium consumption achievable by the EMOX concept, and comparisons have been made of this performance with that of typical MOX and NF fuels. The results indicate that EMOX and NF fuels can provide flexibility for controlling plutonium inventories in spent fuel. In addition, fabrication experiments have be conducted to determine the feasibility of fabricating suitable EMOX and NF fuels. NF and EMOX fuels have been fabricated using the solid-state reaction method. Precursor powders were successfully blended and milled using a combination of ball milling and high-energy vibratory milling. Sintering data for EMOX fuel indicated that significant densification occurred at a temperature of 1700°C.

INTRODUCTION

In 1994, the Committee on International Security and Arms Control (CISAC) was formed under the direction of the National Academy of Science to study the issue of how to manage best several tons of surplus material arising from the dismantling of nuclear weapons in the United States (US) and the Former Soviet Union (FSU). One of the principal recommendations[1] arising from their study was that the two

countries should "pursue long-term plutonium disposition options that: . . . result in a form from which the plutonium would be as difficult to recover for weapons use as the larger and growing quantity of plutonium in commercial spent fuel." The committee recommended two attractive options for achieving this "spent-fuel standard," one of which was the fabrication and use of mixed oxide (MOX) fuel in existing or modified nuclear reactors (the other was vitrification with high-level radioactive waste). Although the implementation of either of these options will serve to alleviate the "clear and present danger" created by the surplus inventories, the need to address the larger issue of the global inventories existing as spent reactor fuel still exists. The committee recognized this need, as is shown in their statement,

> ...consideration of further steps to reduce the long-term proliferation risks of such materials is required, regardless of what option is chosen for disposition of weapons plutonium. This global effort should include continued consideration of more proliferation-resistant nuclear fuel cycles, including concepts that might offer a long-term option for nearly complete elimination of the world's plutonium stocks.

Although the surplus inventories created from the dismantling of nuclear weapons are the most attractive for potential weapons use, the reactor-grade plutonium in spent nuclear fuel is still a potential threat. Figure 1 shows the critical masses of several fissile elements, including plutonium with both weapons- and reactor-grade isotopics. These critical masses were calculated based on a bare, unreflected sphere configuration. There is little difference between the reactor-grade and weapons-grade values. Although the true measure of weapons-quality material is more complicated, this figure demonstrates the attractiveness of spent reactor fuel to potential proliferants. Because the world-wide inventories of reactor-grade plutonium are much greater than weapons-grade material and are in much more diverse locations, the management of this material is an important consideration for reducing proliferation risks.

To address this issue, Los Alamos National Laboratory (LANL) is currently investigating the use of Evolutionary Mixed Oxide (EMOX) fuel for the purpose of better managing plutonium inventories that arise from the use of nuclear power reactors. This EMOX fuel exists in a variety of forms, with its main characteristic being that the fuel matrix contains a nonfertile (NF) component (currently calcia-stabilized zirconia). By replacing part or all of the fertile component (^{238}U) of the fuel, the net change in the plutonium inventory over the fuel cycle can be controlled. This allows EMOX fuel to be used for a variety of purposes: to dramatically reduce existing plutonium inventories through the use of a pure NF fuel (PuO_2-ZrO_2-CaO), to control plutonium inventories in a closed-fuel cycle to minimize excess materials through the use of a less-fertile fuel (UO_2-PuO_2-ZrO_2-CaO), or to minimize the amount of plutonium that must be placed in a geologic repository because of the use of a once-through fuel cycle by using a less-fertile fuel

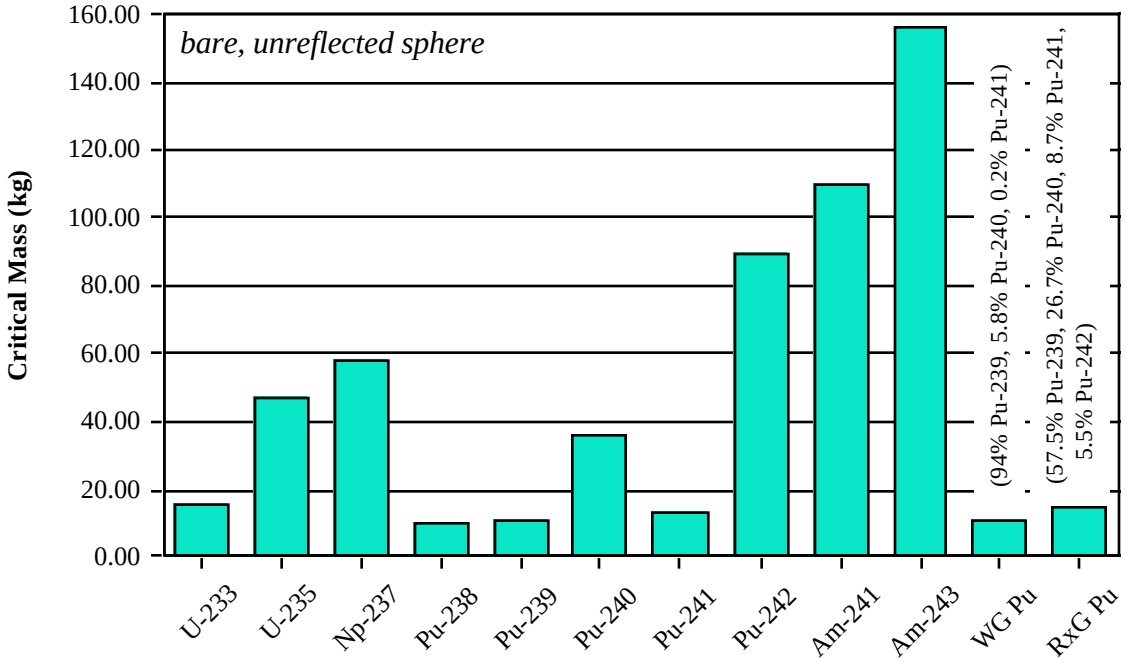

Fig. 1. Critical masses of various fissile elements for bare, unreflected sphere configurations.

(UO_2-ZrO_2-CaO). This report only deals with examination of the plutonium-bearing fuels, although examination of the once-through EMOX fuel is also actively being pursued at LANL.

The approach for the analysis of the EMOX concept consists of three parallel but connected paths. The first path involves the analysis of the concept from a reactor viewpoint, using physics codes in conjunction with certain self-imposed constraints. One major objective of this program is to develop a fuel form that could be used in existing reactor designs. The fuel must also adhere to safety (in-reactor behavior) and economic (fuel lifetime) considerations.

The second path is the assessment of the feasibility of fabricating such a fuel. In the fuel development laboratory at LANL, a program is currently under way to address the issues involved with the fabrication of the EMOX fuels, using both surrogate materials and actual plutonium. The program also includes the examination of such properties as phase distribution, pore size, grain size, and degree of densification. The major constraint is to limit the fabrication process to existing processes, thereby enhancing its commercial acceptability. This effort is closely coupled to the analysis effort to jointly produce a feasible fuel form.

Finally, the third path involves the examination of certain performance metrics. Such metrics include the effect on worldwide (or system-wide) plutonium

inventories, economic impacts, and the use of the energy-potential that exists in the fuel.

FUEL PERFORMANCE

Extensive calculations have been performed to assess the feasibility of incorporating the EMOX fuel form into existing pressurized water reactor (PWR) systems. The amount of plutonium consumption in EMOX has been assessed as a function of several variables, including initial plutonium loading, core fraction and nonfertile fraction. The EMOX performance has been compared with MOX and NF system plutonium inventory changes. The fuel and moderator temperature reactivity coefficients for EMOX have also been calculated and compared with MOX and NF behavior. Finally, initial determination of critical masses of discharged EMOX compositions has been completed.

METHODOLOGY

A PWR pin cell model was developed for use in the HELIOS[2] code. HELIOS is a collision probability based transport code that supports general, two-dimensional geometries. It has the ability to use current coupling between subcomponents, which allows for reduced resource and time requirements. It has the further ability of performing burnup or branch-off calculations and of generating homogenized and/or weighted cross-sections over any designated region. One advantage of this code is its cross-section library, containing over 270 explicit materials and data for 115 fission products. Fuel materials are represented in temperatures up to 2000 K, and other isotopes are represented in the range of 300 to 1200 K.

A typical Westinghouse PWR[3] was used for the model development, and the dimensions used are shown in Table I. Figure 2 shows the computer representation of the pin cell model. The central darker areas represent the three fuel regions, which are created to better enhance calculational performance. The lighter cylindrical area represents the Zircaloy cladding, and the four rectangular areas represent the coolant. This model was used for all calculations, unless otherwise specified.

NOMENCLATURE

Figure 3 attempts to provide a visual description of the nomenclature used in this report. As is done with conventional MOX in a UO_2 core, the envisioned fuel cycle would consist of the addition of some fraction of EMOX (in this case 18.4%) to a standard enriched UO_2 core. This is depicted in the left-most pie chart entitled "Whole Core Composition." The EMOX section of the core will hence be referred to as the "EMOX core fraction." The right-most chart (EMOX composition) depicts a typical composition of the EMOX core fraction. The EMOX composition comprises

TABLE I
PWR PIN CELL MODEL DIMENSIONS

Dimension	Measurement (cm)
pellet radius	0.4095
pin outside diameter	0.94
clad thickness	0.0572
pitch	1.25
height	366.0

Fig. 2. Computer representation of HELIOS PWR pin cell model.

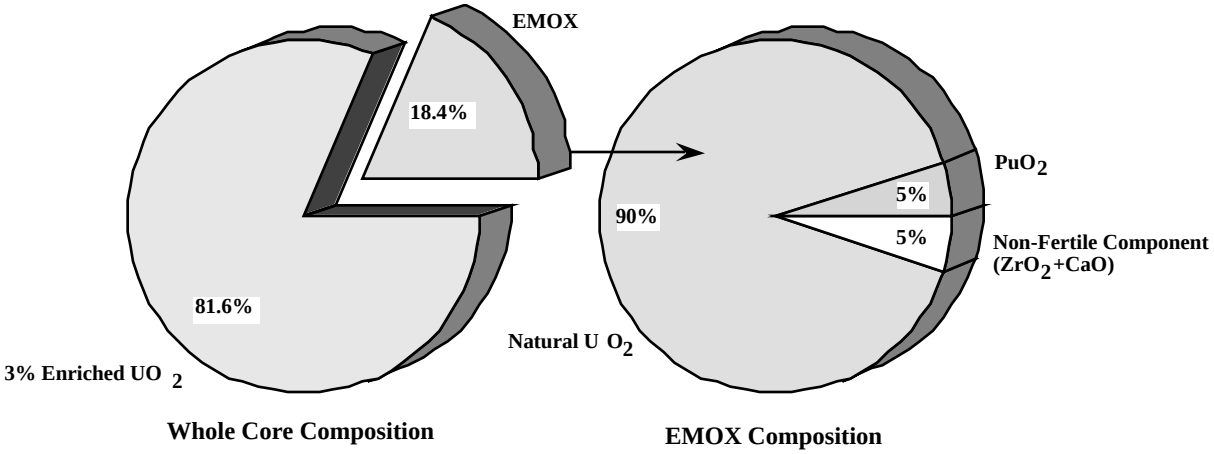

Fig. 3. Nomenclature depiction for EMOX calculations.

varying percentages of PuO_2, natural UO_2 and varying amounts of a nonfertile component of calcia-stabilized zirconia. The amount of this nonfertile component in EMOX is the "non-fertile fraction."

BENCHMARK

To benchmark the methodology, an attempt was made to recreate published results[4] for multiple recycles of standard MOX fuel in a PWR. The PWR pin cell model detailed above was used in conjunction with two different burnup scenarios. The first scenario utilized the 30,400 MWd/MTHM burnup and 37.0 MW(t)/MTHM power rating specified for the reference results.[4] The second scenario utilized the burnup (33,000 MWd/MTHM) and specific power (37.8 kW/kg), which are typical reference values used when performing PWR modeling calculations.[3] The distribution of the plutonium isotopes for each case were calculated as discharged from the first reload of 3% enriched UO_2 fuel, and these results are shown in Fig. 4 in conjunction with the previously published results. The calculational results compare closely to these, with the major difference arising in the ^{240}Pu percentages.

These results were then used as a basis for multiple MOX recycles following the reference loading scheme. The results of the two differing-burnup calculations are shown in Fig. 5 in the form of the critical mass of the resultant composition discharged from each recycle. The critical mass was calculated from the plutonium isotopic composition for a bare, unreflected sphere, and is one measure of the proliferation resistance of the resultant fuel. Although the isotopic distributions do differ slightly, little difference is reflected in the corresponding critical masses.

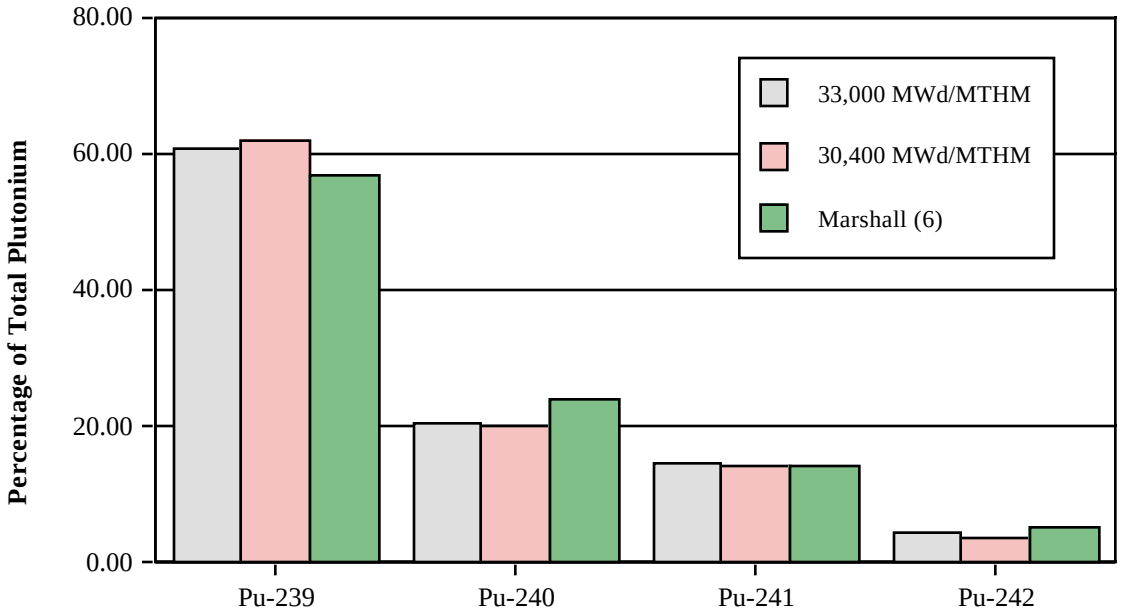

Fig. 4. Comparison of results for UO_2 discharge plutonium compositions.

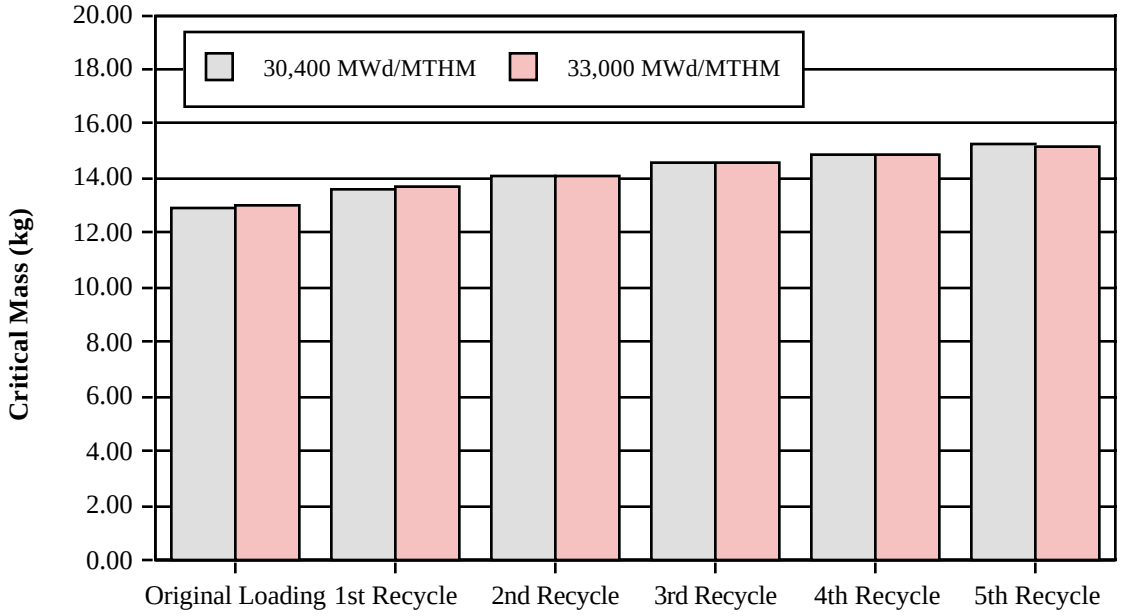

Fig. 5. Critical masses of plutonium compositions discharged from MOX recycles.

PLUTONIUM CONSUMPTION IN EMOX

There are several variables of importance when performing analyses such as the desired EMOX calculations, all of which will be examined in this section. These variables include the fraction of the core that is loaded with the new fuel form, the initial plutonium loading in the EMOX component, and the nonfertile fraction used in each composition. The first parameter to be examined here in the EMOX plutonium consumption calculations was the effect that varying the EMOX core fraction has on reactor performance, keeping a constant nonfertile fraction (30%). Calculations were performed using varying (5, 10, and 15%) PuO_2 loadings, while varying the EMOX core fraction from 10 to 100% for each case. Also included in the calculations were pure MOX cases (no nonfertile fraction) with 5 and 10% PuO_2 loadings. The percent of change in plutonium inventories (from beginning- to end-of-life) for each case is plotted in Fig. 6. The higher plutonium loadings require lower core fractions to become converter cores (around 40% for the 5% PuO_2 loading and just under 20% for the 20% PuO_2 loading).

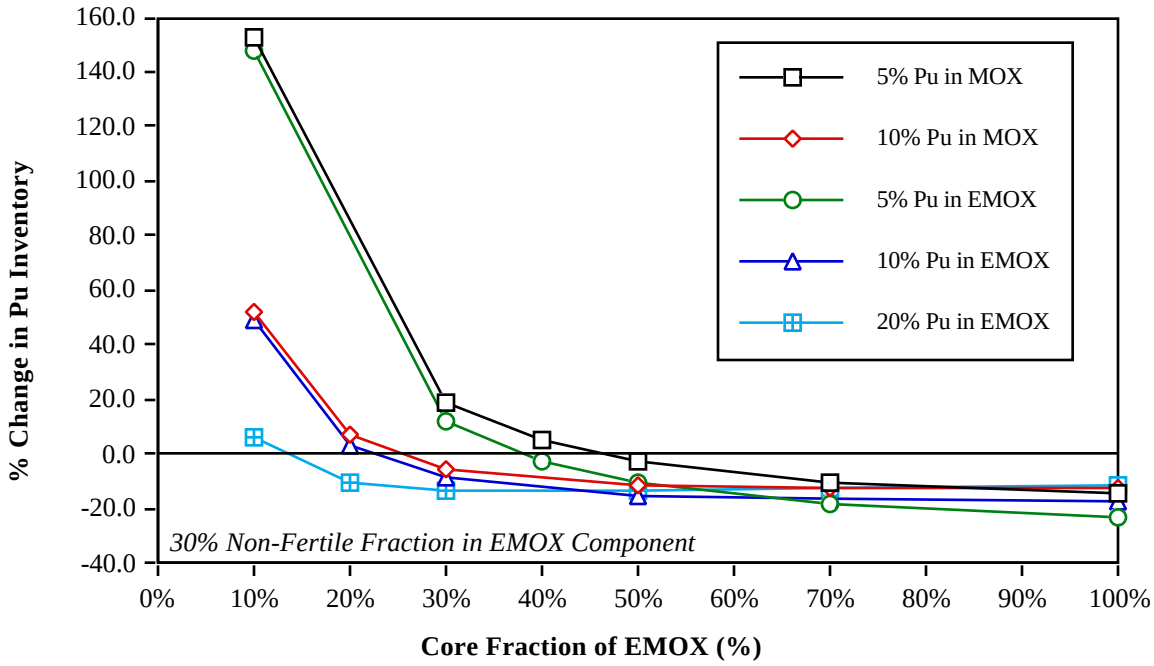

Fig. 6. Plutonium inventory change as a function of EMOX core fraction and initial plutonium loading.

The next set of calculations further investigated the effect that varying the initial plutonium loading has on EMOX performance. The results were again compared with similar MOX cases, as shown in Fig. 7, for third- and full-core configurations. Again, in the EMOX cases, the nonfertile fraction was held to 30%. The EMOX cores show an advantage over the pure MOX cores. For the third-core configurations, the EMOX core becomes a plutonium converter at an initial plutonium loading of ~6%, whereas the MOX core does not become a converter until the plutonium loading is increased to ~8%. The full EMOX core appears to be a converter for all plutonium loadings, and exhibits a performance "maximum" at ~3%.

We then wanted to see the effect that varying the NF fraction would have on the EMOX behavior. The next set of calculations, therefore, varied the NF fraction for third-, half- and full-core EMOX configurations. The scope of interest for the NF fraction ranges from zero (pure MOX) to all (pure NF, no UO_2 component in the EMOX), with selected increments in between. The core composition utilized for these calculations reflected a more realistic implementation scenario in that a third of the core was fresh fuel, a third was once-burned fuel, and the remaining third was twice-burned fuel.

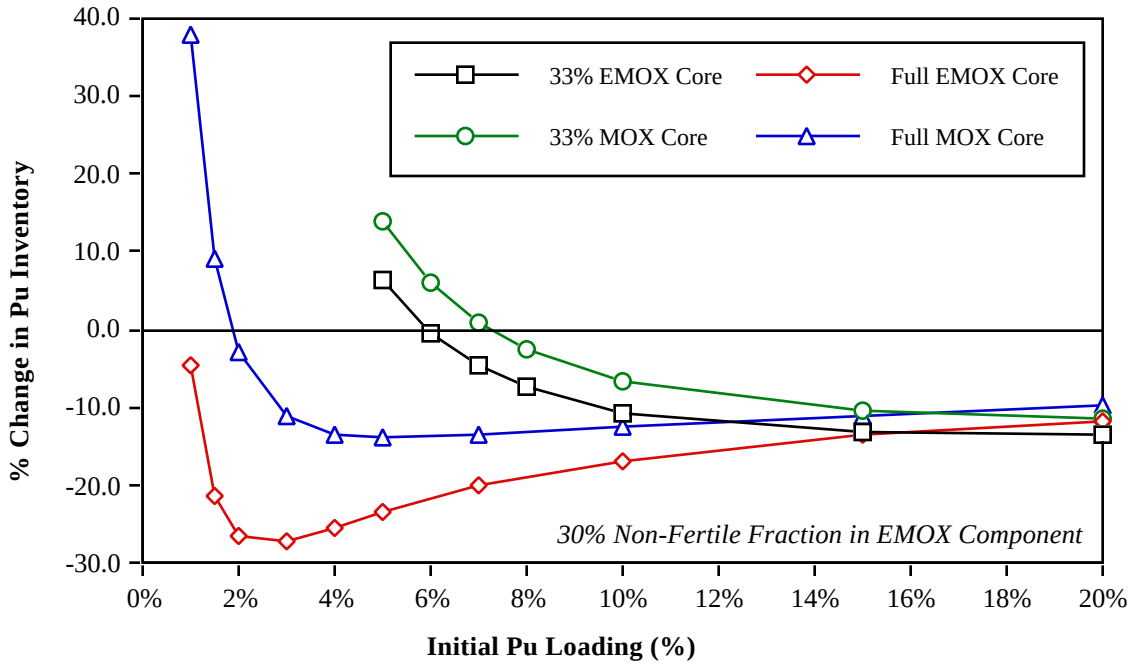

Fig. 7. Change in plutonium inventory for EMOX and MOX core configurations as a function of initial plutonium loading.

Figure 8 presents the third-core results in the form of percent change in plutonium inventory as a function of initial plutonium loading for the various compositions. The point at which each composition becomes a plutonium converter varies, ranging from ~3.5% for the pure NF case to ~7% for the pure MOX case, with the EMOX cases spanning the gap between the two extremes. Greater performance differences between compositions is achieved at lower plutonium loadings. It is also of interest to note the convergence of the curves at the higher plutonium loadings (20%). For this case, all of the compositions remain critical for the duration of the fuel lifetime.

Figure 9 presents the results from similar calculations performed for a half-core configuration. These compositions require lower initial plutonium loadings (as compared with the third-core cases) for each composition to become a converter. The values range from just under 1.5% for the pure NF case to ~4.5% for the pure MOX case. Greater destruction percentages are achieved through the use of a half-core as opposed to a third-core configuration, and the curves again converge at the higher plutonium loadings. Again, for this case, all compositions remain critical for the duration of the fuel lifetime.

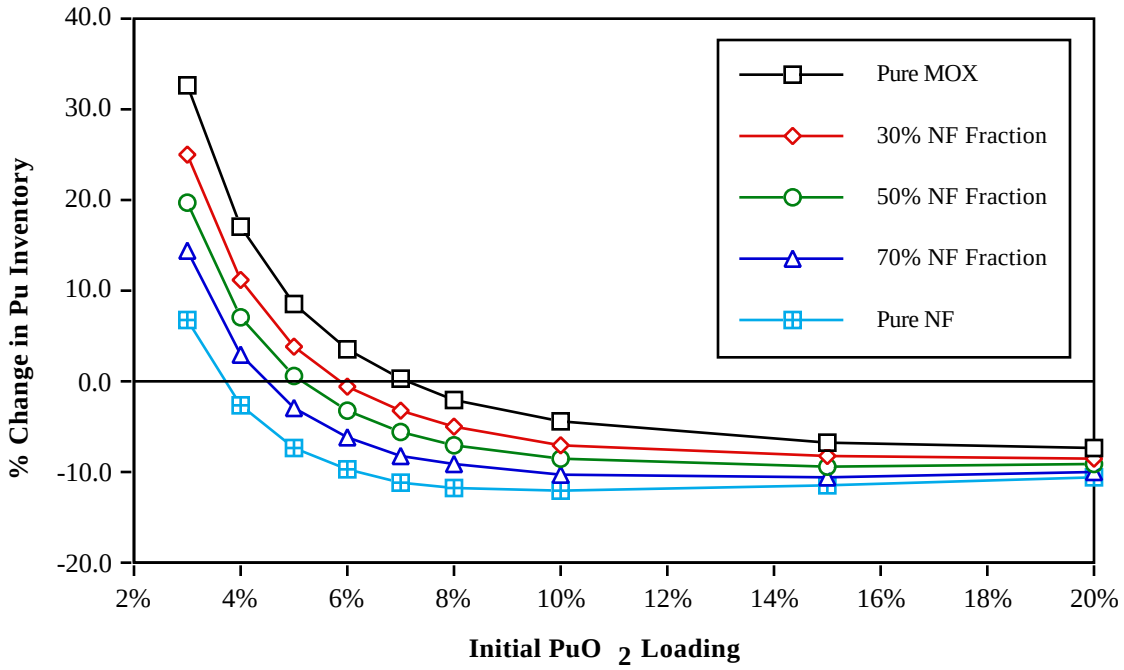

Fig. 8. Change in plutonium inventory for various third-core EMOX compositions as a function of initial plutonium loading.

Finally, Fig. 10 presents the full-core comparison results. Significantly higher destruction percentages are achieved, and all the selected EMOX cases are converters over the entire plutonium loading range. Performance maximums can be seen at the lower plutonium loadings for the EMOX cases. Only the compositions with initial plutonium loadings of >3%, however, remain critical for the duration of the fuel lifetime. The pure NF cases with <3% plutonium burn up completely before they reach the predetermined fuel lifetime of 873 days.

Overall, varying the nonfertile component in EMOX fuel compositions has the greatest effect at lower plutonium loadings and higher core fractions. The pure NF cases provide the best performance, with the EMOX cases spanning the gap between that and the pure MOX boundary.

COMPARISON OF EMOX TO MOX AND NF FUELS

The next series of calculations involved the comparison of the EMOX and NF concepts with typical MOX fuels under the same irradiation conditions. The three fuel forms were examined in both third- and full-core configurations.

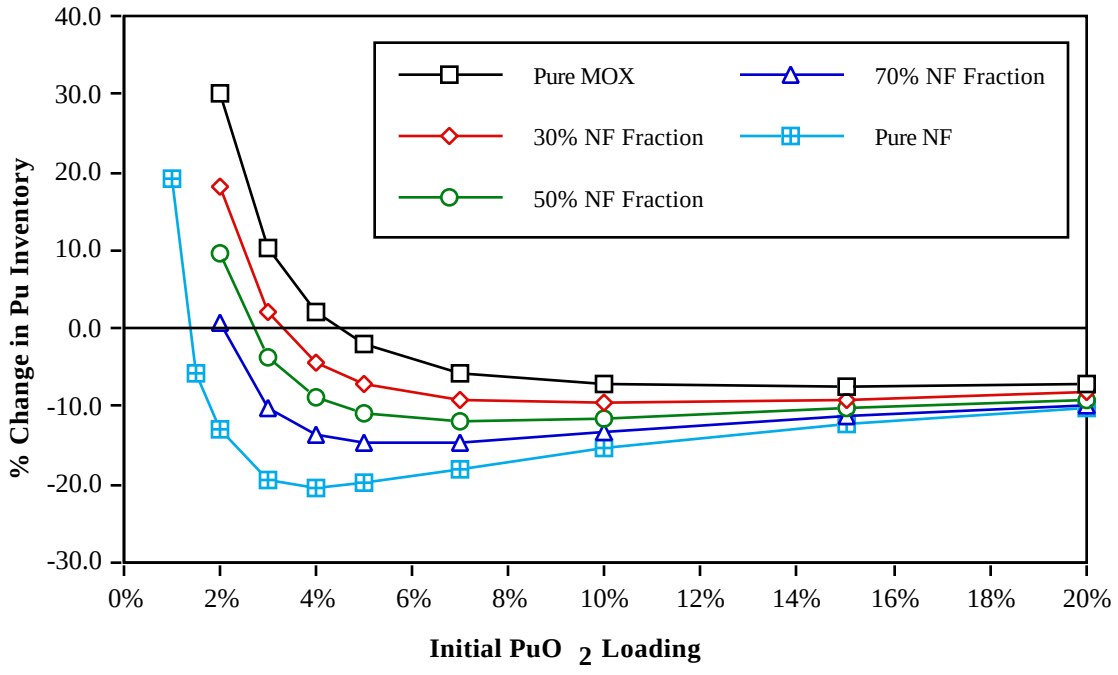

Fig. 9. Change in plutonium inventory for various half-core EMOX compositions as a function of initial plutonium loading.

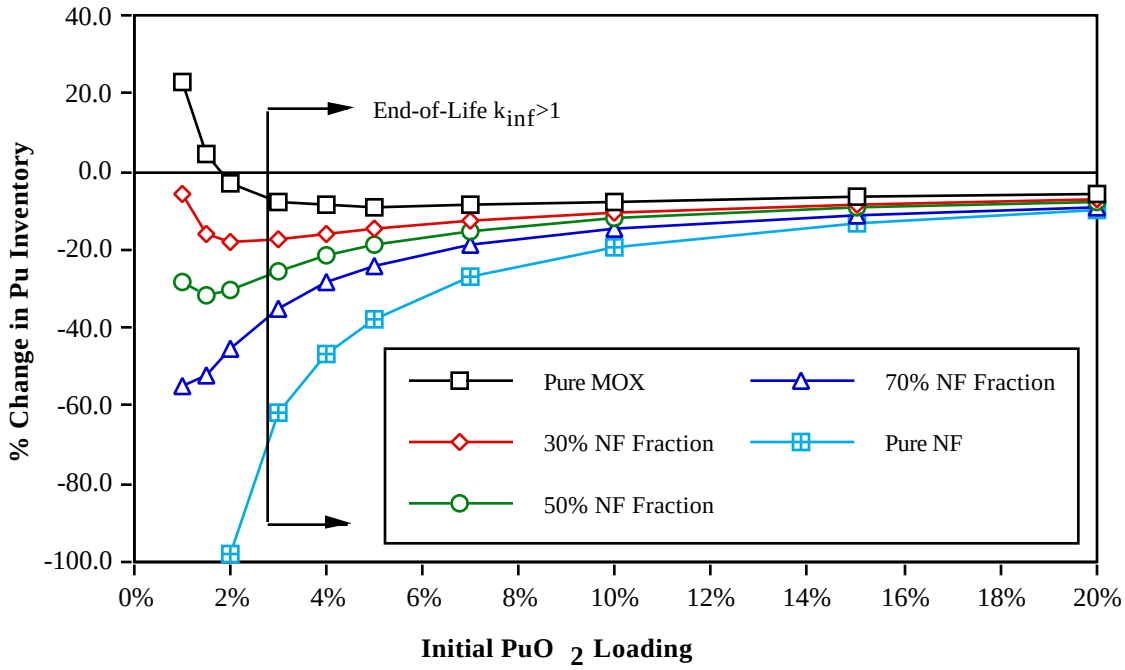

Fig. 10. Change in plutonium inventory for various full-core EMOX compositions as a function of initial plutonium loading.

Figure 11 shows the percent change in the plutonium inventory over the fuel lifetime (873 days) for selected MOX, EMOX, and pure NF cases. The 33% MOX core represents a European MOX core loading. In all cases, there was an initial plutonium loading of 6% within the MOX component (MOX, EMOX, or NF), and in all third-core cases, the remainder of the core was 3% enriched UO_2. The MOX comprises strictly PuO_2 and natural UO_2. The EMOX component comprises PuO_2, UO_2, and ZrO_2-CaO, whereas the NF cases contained only the PuO_2-ZrO_2-CaO mixture. In the EMOX cases, the nonfertile fraction was held to 30%, whereas in the NF cases, the nonfertile fraction was the remainder of the MOX component minus the plutonium oxide loading.

In Fig. 11, the typical European MOX core would be a breeder of plutonium if it had a plutonium loading of 6%, whereas if the same core fraction (33%) were dedicated to EMOX, it would become a converter of plutonium (albeit slightly). As expected, the NF cases produce more dramatic results because there is initially significantly less uranium present for breeding, or none present, as in the full NF core case.

Figure 12 plots the data for the same cases in the form of the core-averaged single pin plutonium inventory over the fuel lifetime. The third-core loadings initially have a much lower plutonium inventory as compared with the full-core cases. The EMOX shows a slight advantage over the pure MOX cases, and the performance of the NF case, particularly the full-core case, again is amplified.

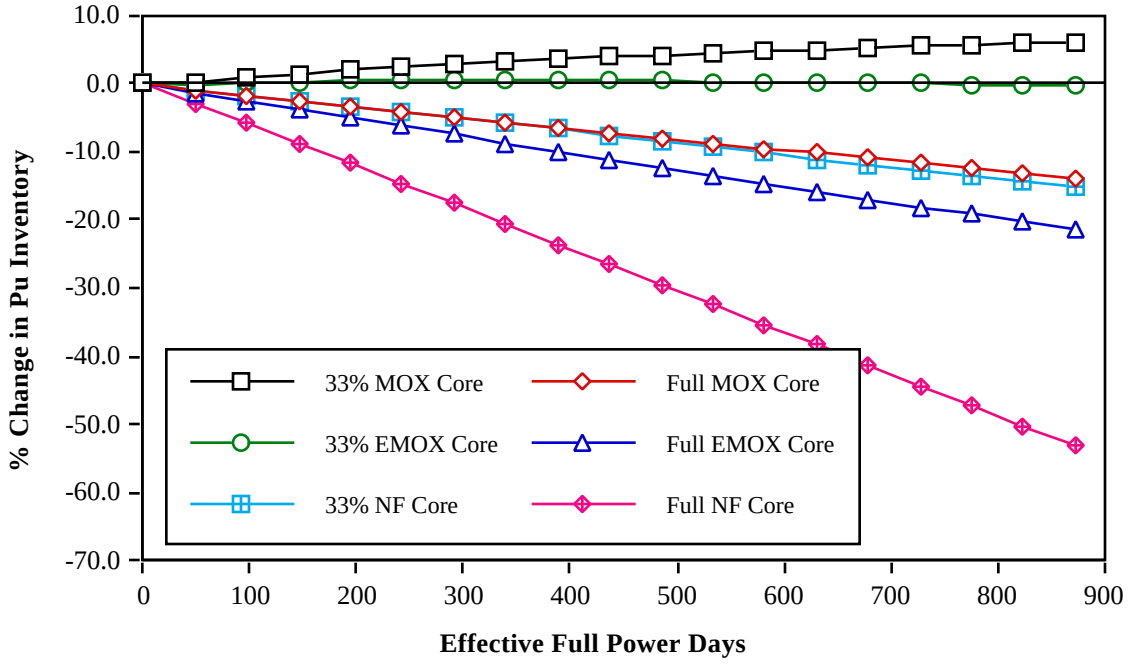

Fig. 11. Change in plutonium inventory over fuel lifetime for various fuel forms (6% PuO_2).

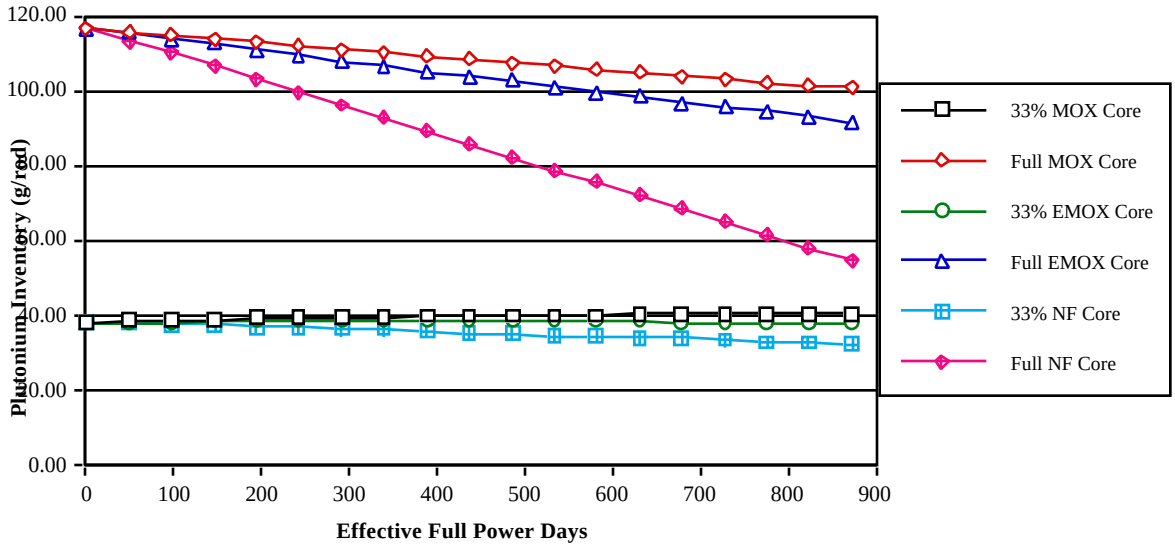

Fig. 12. Plutonium inventory over fuel lifetime for various fuel forms (6% PuO_2).

TEMPERATURE REACTIVITY COEFFICIENTS

A preliminary assessment of fuel and moderator temperature reactivity coefficients for various EMOX fuel compositions was performed. A similar assessment was also performed for select MOX and NF compositions. The temperature coefficients were calculated from the initial system criticality using Eqn. (1):

$$\frac{(k_2 - k_1)}{(k_1)(T_2 - T_1)} \tag{1}$$

where k_1 is the initial multiplication factor for the cell, k_2 is the multiplication factor after the change in temperature, T_1 is the initial temperature, and T_2 is the final temperature.

The original pin cell model consists of three separate fuel regions, as shown in Fig. 2. There were, therefore, three corresponding fuel region temperatures, which raised the question of how best to perform the temperature coefficient calculations. For this initial assessment, the model was reconfigured to contain an average fuel temperature that could be varied, so that the new average temperature would be applied simultaneously to all three fuel regions.

The first set of calculations involved varying the initial plutonium loadings while using a constant NF fraction of 30%. Figure 13 shows the resultant temperature coefficients for the 33% EMOX case for PuO_2 loadings from 5 to 20%. (Note: reactivity coefficient calculations with the 33% EMOX core only make sense if the UO_2 pellets were to be homogeneously distributed with the EMOX pellets, which

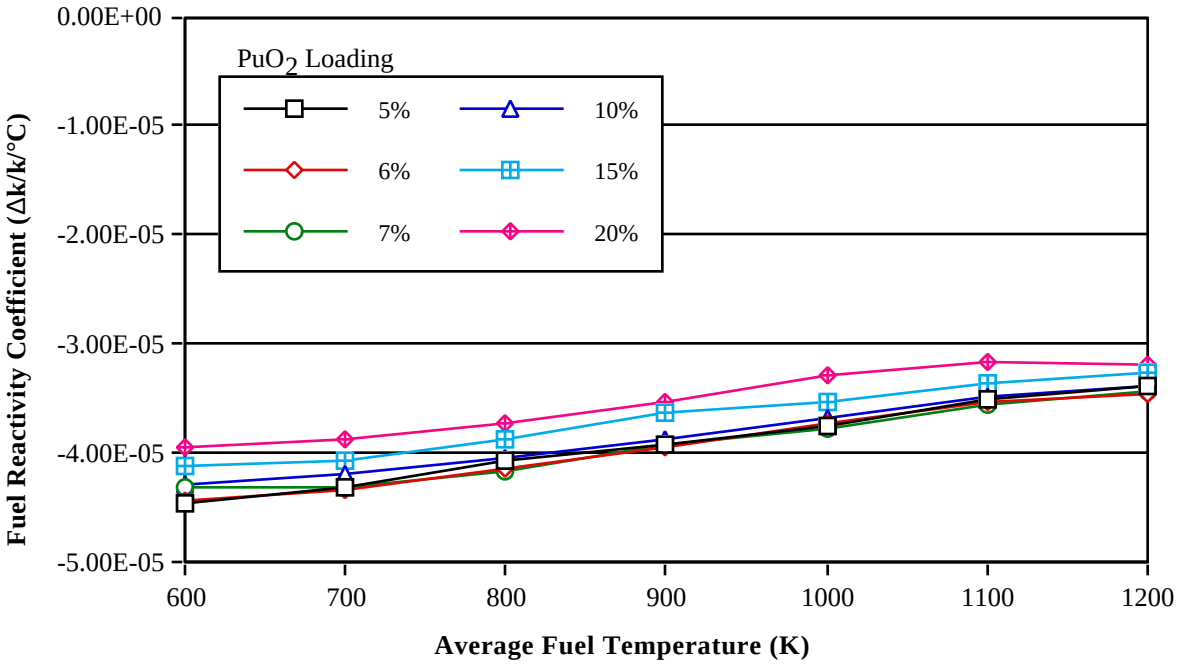

Fig. 13. Fuel temperature reactivity coefficients for third-core EMOX composition as a function of initial plutonium loading.

would be unlikely in actual implementation.) These are all negative and the absolute magnitude decreases with increasing plutonium loading.
Figure 14 shows the results of the same calculations performed for the full EMOX core, varying the PuO_2 loadings from 1 to 20%. The 20% case exhibits anomalous behavior as compared with the remaining curves. As of yet, no explanation for this behavior has been found. It is thought to be a manifestation of the code, but a definitive explanation requires further investigation.

The fuel temperature reactivity coefficients for the various fuel forms (MOX, EMOX, and NF) examined in Fig. 11 were analyzed, and the results are found in Fig. 15. The coefficients for the third-core cases for all three fuel forms behaved similarly, all negative and with the absolute magnitude decreasing with increasing temperature. The full-core MOX and EMOX cases also behave similarly, while the full-core NF case's coefficients are much greater, but still negative. Although there is a complete absence of uranium in the pure NF case, the ^{240}Pu isotope has a capture resonance at 1 eV, which is the dominant contributor to the negative behavior of this case.

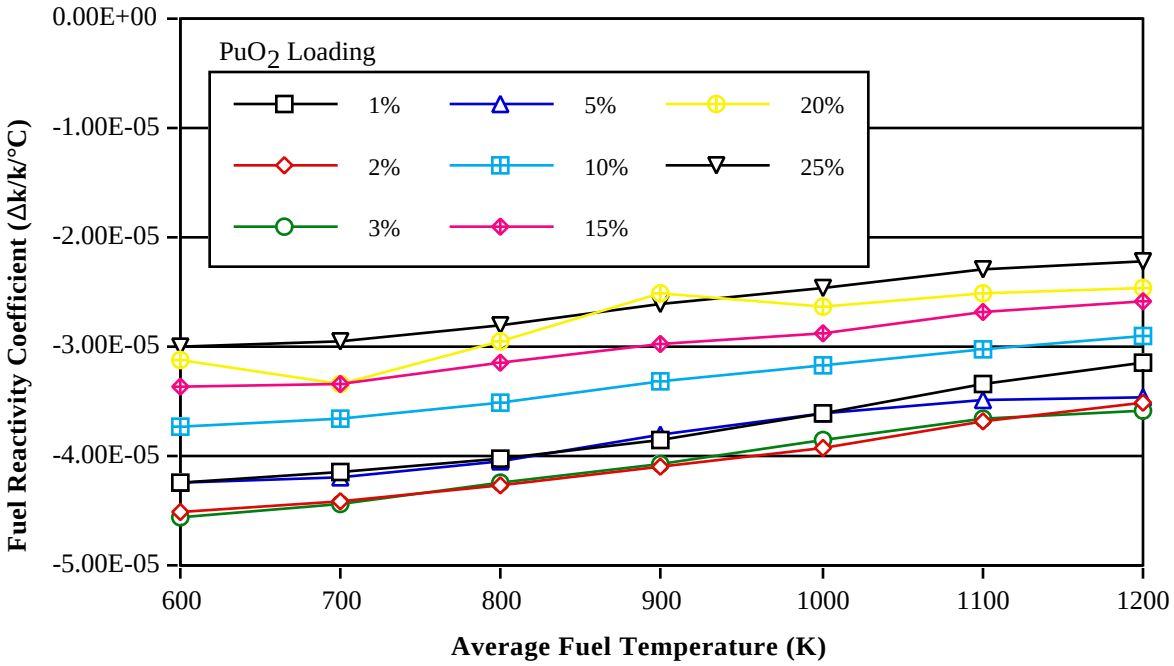

Fig. 14. Fuel temperature reactivity coefficients for full-core EMOX composition as a function of initial plutonium loading.

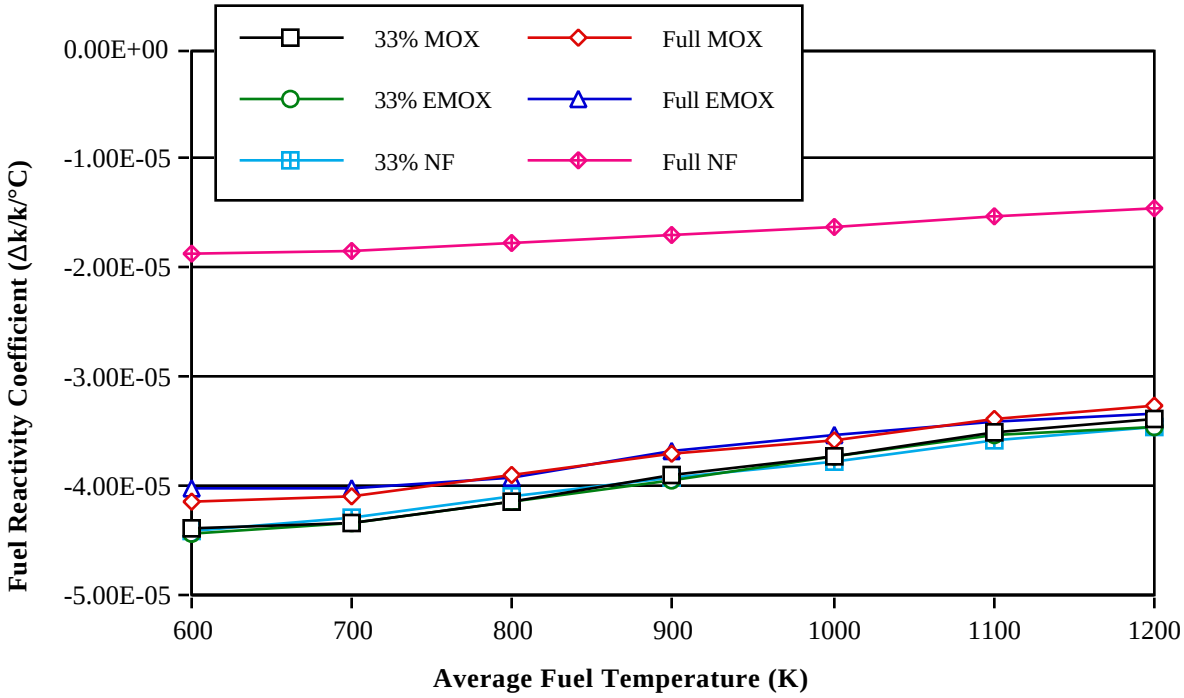

Fig. 15. Fuel temperature reactivity coefficients of various fuel forms (6% PuO_2).

The moderator temperature reactivity coefficients were also calculated from the initial system criticality using Eqn. (1), with the criticality being determined by moderator density changes because of temperature variations. For the most part, the same cases were analyzed as those done for the fuel coefficients; the same pin cell model was used throughout.

Figure 16 shows the reactivity coefficients obtained from varying the initial PuO_2 loading for the third-core EMOX case from 5 to 20%. The coefficients become less negative with increased plutonium loading but are still negative over the temperature range for all cases, and decrease with increasing temperature.

Figure 17 shows the coefficients obtained from varying the initial plutonium loading (from 1 to 20%) for the full-core EMOX case. These coefficients are less negative as compared with the third-core results. At the higher plutonium loadings, the coefficients tend to not decrease as much with increasing temperatures. For the 20% PuO_2 case, the coefficients are positive for a significant portion of the temperature range.

Finally, Fig. 18 shows the moderator reactivity coefficients obtained from the comparison of the EMOX compositions to those of MOX and NF, for both third- and full-core configurations. The coefficients for the third-core cases behave similarly, all negative, and become more negative with increasing temperatures. The full-core

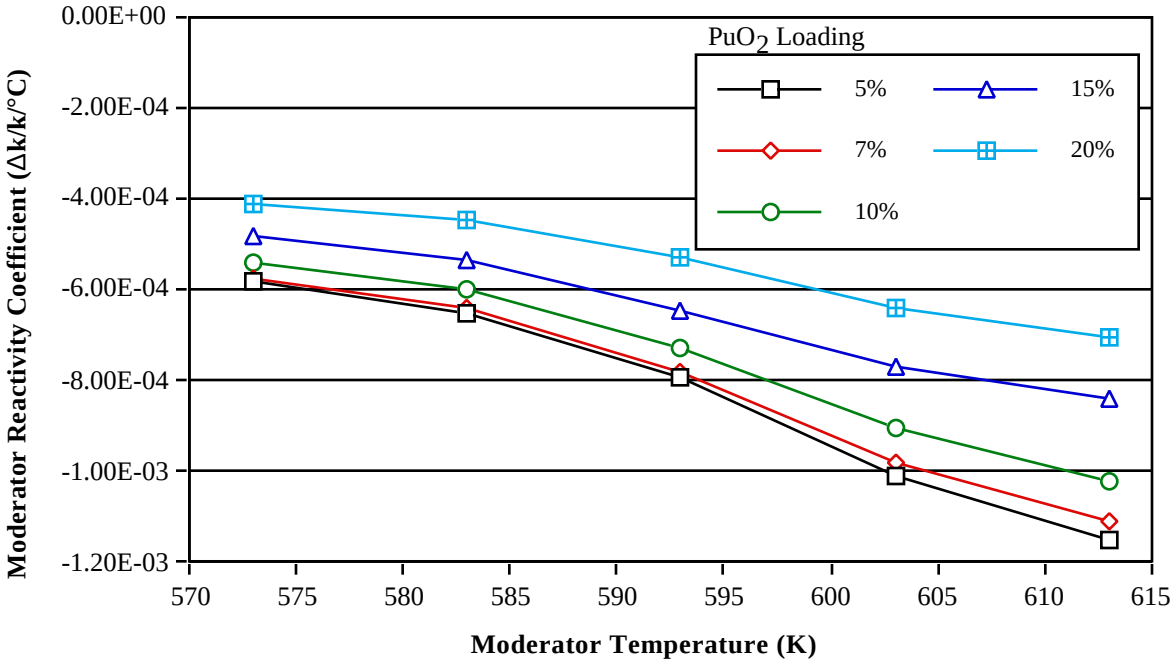

Fig. 16. Moderator temperature reactivity coefficients for third-core EMOX case as a function of initial plutonium loading.

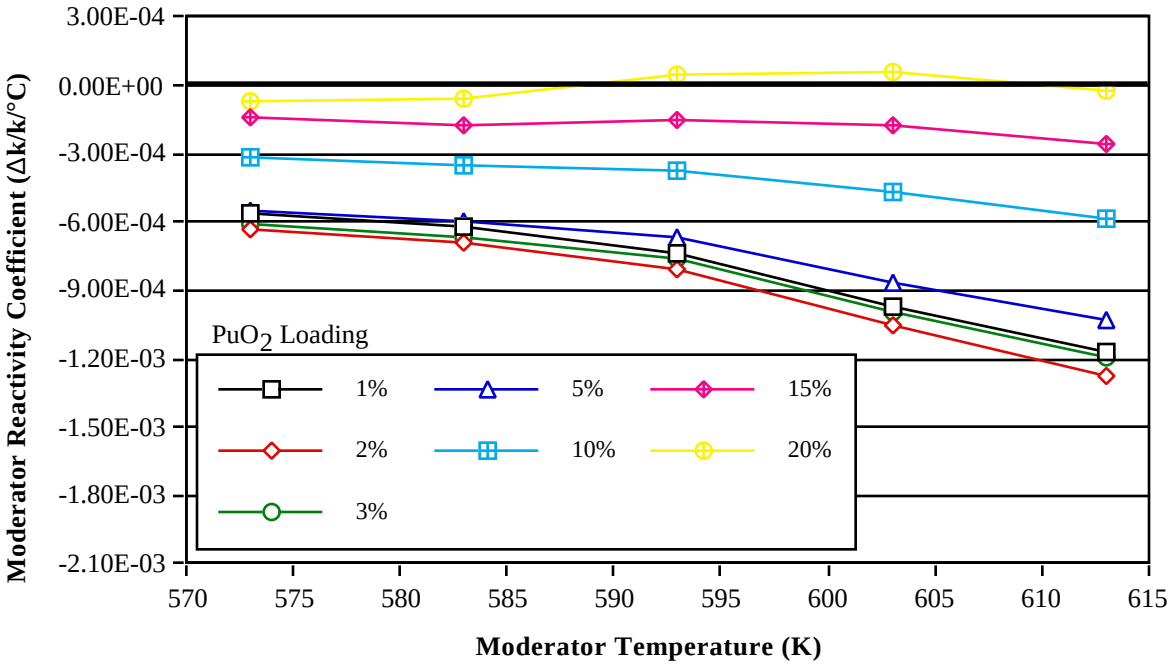

Fig. 17. Moderator temperature reactivity coefficients for full-core EMOX case as a function of initial plutonium loading.

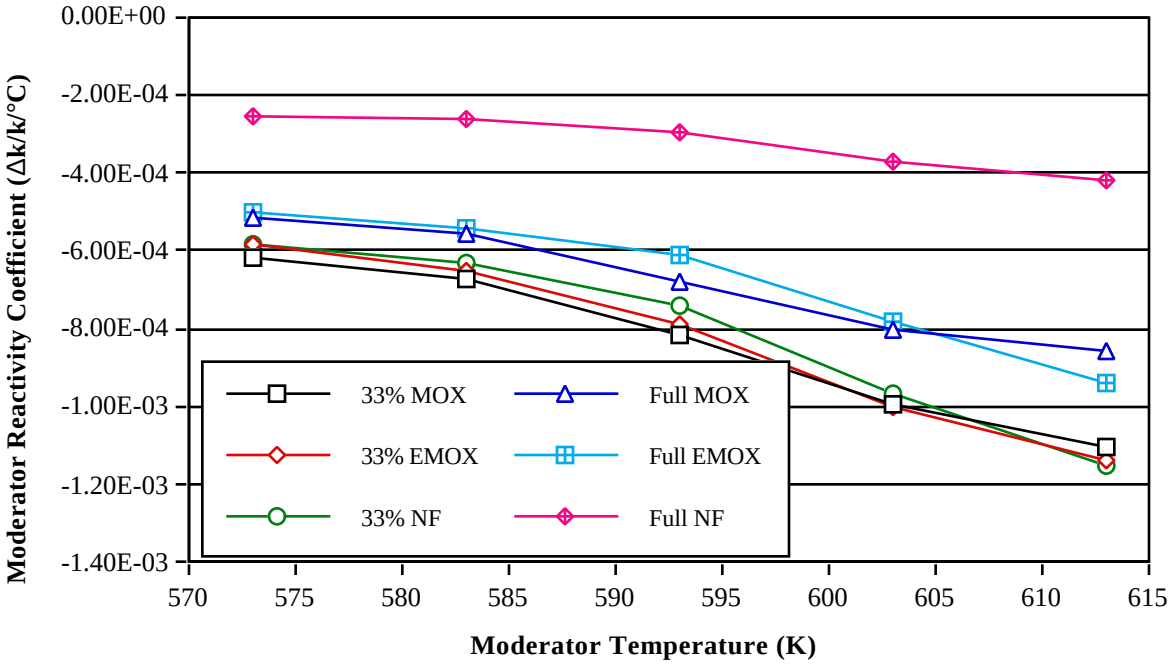

Fig. 18. Moderator temperature reactivity coefficients of various fuel forms (6% PuO_2).

MOX and EMOX also behave similarly, as expected. Although the NF case's coefficients are smaller in magnitude, they are still negative over the moderator temperature range.

Overall, the EMOX fuel temperature coefficients behave similarly to those for MOX and EMOX fuels; therefore, they could be expected to behave similarly to MOX fuel with respect to temperature changes during irradiation.

CRITICAL MASSES

The critical mass of varying isotopic compositions can be calculated using a bare, unreflected sphere configuration. This critical mass is one measure of the proliferation resistance of the resultant fuel form. Critical mass calculations were performed for several of the aforementioned configurations, and a select few are highlighted below. A true measure of proliferation resistance requires a more detailed assessment, which will be performed once a suitable fuel form has been better defined.

Figure 19 shows the critical masses of the resultant isotopics from the cases previously examined in Fig. 6. In these cases, the percent change in plutonium inventory was calculated as a function of EMOX core fraction and initial plutonium loading. As shown in Fig. 19, the critical masses do not differ significantly over the five cases. While the EMOX and MOX cases with 5% PuO_2 loadings have the largest critical masses, and increase with increasing core fraction, the EMOX case values are much larger at the higher core loadings. The 10% PuO_2 EMOX and MOX cases have greater critical masses at lower core fractions but actually decrease at loadings higher than ~30%. Finally, the 20% PuO_2 EMOX case has the largest critical mass initially and reaches its maximum value at a 20% core fraction.

Critical masses were also calculated for the cases presented in Fig. 7, and the results are presented in Fig. 20. In this scenario, the percent change in plutonium inventory was calculated as a function of initial plutonium loading for third- and full-core EMOX and MOX configurations. As seen in Fig. 20, the critical masses decrease as the plutonium loading increases. This decrease is more dramatic in the full-core cases, especially at the lower plutonium loadings.

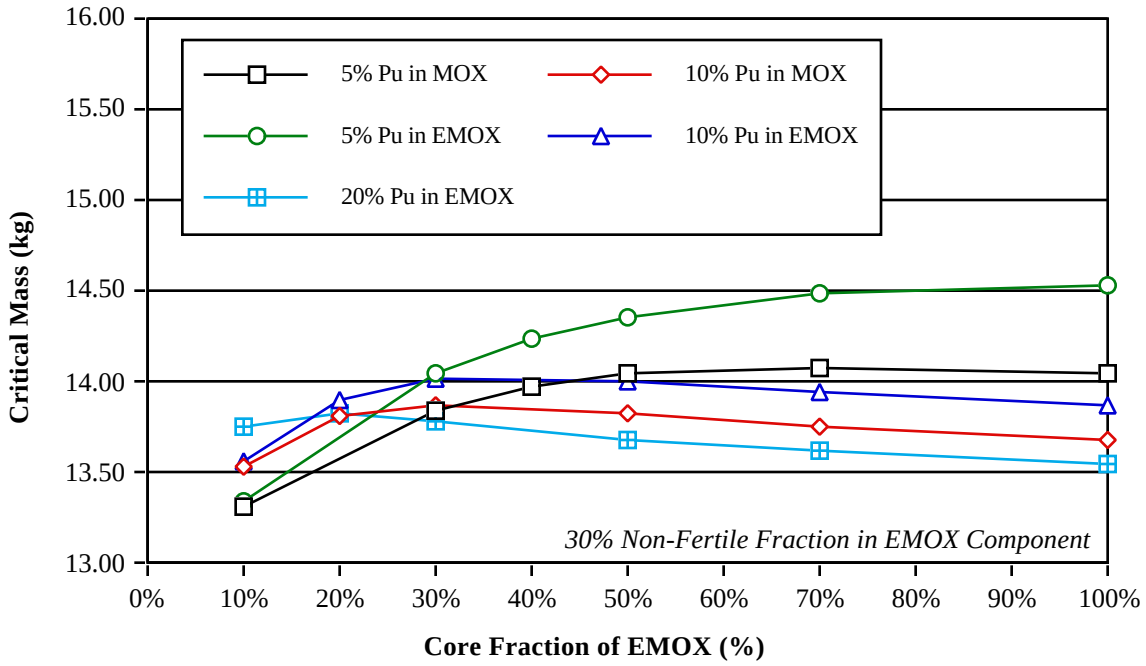

Fig. 19. Critical masses of discharged plutonium inventories as a function of EMOX core fraction and initial plutonium loading.

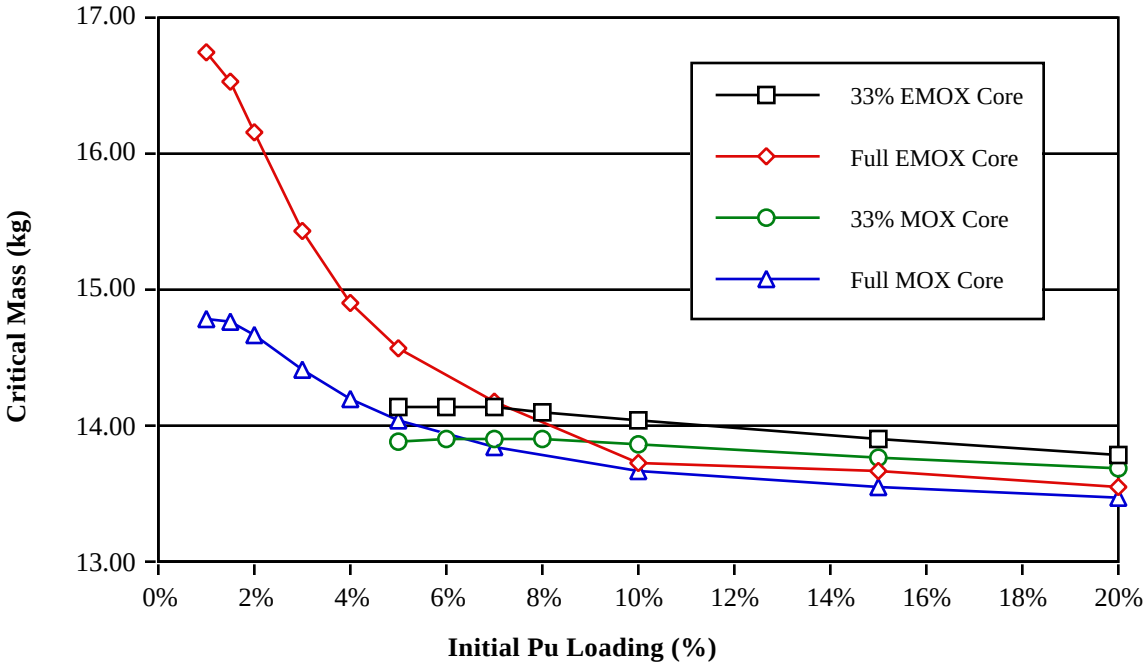

Fig. 20. Critical masses of EMOX and MOX core configurations as a function of initial plutonium loading.

Finally, critical masses were used to present the performance of EMOX over multiple recycles. A 30% EMOX core case with an initial PuO_2 loading of 10% and a NF fraction of 30% was chosen, and five recycle calculations were performed. The plutonium inventory at beginning- and end-of-life remains the same with a constant core fraction and plutonium loading, but the plutonium isotopic distribution changes with each recycle step. Hence, critical masses were an effective method of presenting the results (the corresponding critical mass for the discharged plutonium at each recycle step) shown in Fig. 21. As expected, the critical mass increases, albeit slightly, with each recycle.

FUEL FABRICATION DEMONSTRATION

Introduction

A parallel effort is currently under way to assess the feasibility of fabricating both the NF and EMOX fuel concepts. The majority of the fabrication work is being performed at the Plutonium Facility at LANL. This effort is designed to address the issues involved with the development of a complete fabrication process for these fuel concepts, including the examination of such final sintered fuel pellet properties as phase distribution, pore size, grain size and degree of densification. The entire fabrication process should be demonstrated using cerium oxide (CeO_2) as a surrogate for plutonium to efficiently and cost effectively identify and address preliminary issues and/or potential problems. It is best to perform the entire operation, staying within the guidelines of existing processes, using weapons-grade plutonium. This section, therefore, summarizes the progress made to date on the NF/EMOX fabrication effort.

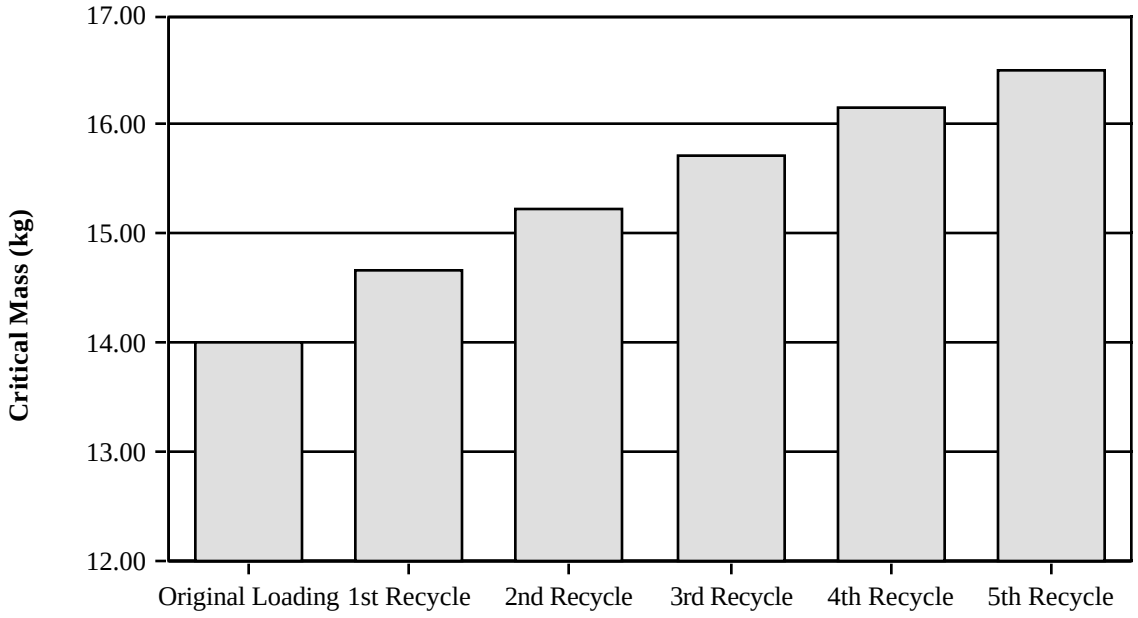

Fig. 21. Critical masses of discharged plutonium inventories for 30% EMOX core and 10% PuO_2 loading recycle cases.

The original focus of this effort was on the pure NF fuel, and most of the results achieved to date are from the demonstration of this concept. By definition, NF fuel is plutonium oxide in a calcia-stabilized zirconium oxide matrix (PuO_2-ZrO_2-CaO). Studies performed at INEL[5] showed that the addition of a depletable neutron absorber (such as erbium, as Er_2O_3) helps to control the initial excess reactivity found in such a system while also enhancing the negative fuel temperature reactivity coefficients, thereby increasing the safety of the system. INEL has also suggested the possible substitution of yttria (Y_2O_3) for calcia as the zirconium stabilizer.[5] This effort will focus on the fabrication of these fuel forms, as well as the variations on the EMOX concept (PuO_2-UO_2-ZrO_2-CaO).

The purpose of the surrogate study was to fabricate a CeO_2-ZrO_2-CaO fuel, which has several applications to the larger effort. Overall, the feasibility of preparing the fuel by the solid-state reaction method using reagent-grade calcia, zirconia, and ceria as oxide precursors was determined. The study served to develop a powder comminution methodology acceptable to glovebox operations while also determining the specifications for a sintering furnace design and operation. Finally, the study provided a cost-effective means of evaluating the behavior of the plutonium oxide in the fuel diluent through the use of the cerium oxide as the actinide surrogate.

Chemical analysis is an essential part of the fuel fabrication process because elemental stoichiometry must be maintained during processing for the fuel to meet fabrication specifications. The development of NF and EMOX fuel has created a need to develop an analytical technique for determining the concentrations of plutonium, uraniam, zirconium, calcium, and erbium in the precursor feed powder and sintered fuel pellet. As part of the overall fuel fabrication effort, a study was initiated to determine the feasibility of using x-ray fluorescence (XRF) analysis to measure the concentrations of the major chemical elements in the fuel. The efficiency of the powder batching process and sintering behavior of the fuel can be determined using this technique of elemental analysis.

BACKGROUND

Fuel Fabrication

The decision to use the ZrO_2-CaO matrix as the fuel diluent was made based on the substantial amount of information published from previous developmental and experimental programs. Unstabilized zirconium oxide by itself is not a viable diluent form. Experience shows that irradiation of UO_2-ZrO_2 fuel will result in rapid densification or void collapse because of phase transformation.[6,7,8] The addition of a small amount of calcium oxide will stabilize the face-centered cubic structure so that it will remain stable under irradiation conditions. This face-centered cubic structure also permits greater solubility of the plutonium oxide in the diluent.

Extensive experimental work has been performed on a uranium ternary fuel (UO_2-ZrO_2-CaO).[9] In the Shippingport PWR, side-by-side irradiation was performed on ternary (UO_2-ZrO_2-CaO), binary (UO_2-ZrO_2), and uranium oxide (UO_2) plate-type elements. The UO_2 and ternary fuels performed similarly, with no reported fuel failures. The binary fuel, however, exhibited rapid densification because of the induced phase instability. Solid ternary fuel pellets were irradiated at the Power Burst Facility, a transient test reactor, and no fuel rod failures occurred with >1000 h of operational experience. Finally, the Light Water Breeder Reactor Fuel Development Program performed side-by-side irradiation of ternary, binary, and UO_2 duplex fuel pellets (annular pellets with thorium center for breeding). Again, the UO_2 and ternary fuels performed similarly, both being successfully irradiated to high burnup. This experimental work not only provided valuable irradiation data, but also developed a substantial base of fabrication and reprocessing technologies for this ternary fuel.

X-Ray Fluorescence Analysis

Conventional elemental analysis has been performed using both XRF and inductively coupled plasma (ICP) spectrometry. These techniques use both optical and mass detector systems. Historically XRF and ICP techniques have utilized sample dissolution and separation of the actinide elements to determine the concentration of the low and trace level elements present in the sample. Although this method is reliable, it is time consuming and can experience problems in dealing with refractory oxide compounds such as zirconium oxide. A direct analysis approach would eliminate dissolution difficulties and provide more reliable results because all analytes would be in the specimen.

ICP can provide direct analysis of the desired analytes of NF and EMOX fuels. Typical XRF sample preparation methodology involves mixing the powder sample with a binder and pressing the mixture into a pellet. This methodology has been shown to produce highly accurate and precise analyses when the standards match the unknown samples. The pellet procedure insures consistent specimen production. The major disadvantage is that the particle size of the standards and unknowns must be assured to minimize any heterogeneity effects that would cause problems in the determination of the analytes.

Compared with analytical techniques requiring chemical dissolution, the use of direct XRF analysis offers several advantages for elemental analysis. These advantages include the ability to (1) perform total sample analysis, (2) reduce time required for sample analysis, (3) minimize waste, (4) recycle specimen pellets, and (5) minimize contamination risks. In each case there are strong benefits of direct analysis. Because the total sample is in the specimen pellet, there is no loss of analyte because of incomplete digestion of the sample. This is important because zirconium is a refractory element and has been known to cause difficulties in dissolution schemes. Reducing the time required for sample analysis is achieved by

eliminating the time for consuming dissolution and chemical separation steps. Because the sample dissolution and separation steps are eliminated, the associated acid and column separation wastes are eliminated as well. Although the oxide powder is mixed with an organic binder, the oxide can be easily separated from the binder and reused for fuel pellet production. Finally, because the pellets are essentially solid materials with good mechanical stability, the risk of contamination from particle dispersal is minimized.

EXPERIMENTAL PROCEDURE

Powder Characterization

For this characterization step, several factors were examined including average particle size, particle size distribution, specific surface area, and impurity levels (through chemical analysis). The equivalent spherical diameter and particle size distribution were determined using laser diffraction analysis and scanning electron microscopy (SEM). The specific surface area was characterized using the BET method. The concentration of gallium in the weapons-grade plutonium was determined by XRF spectrometry.

Fuel Pellet Fabrication

The flow diagram for the surrogate pellet fabrication process is shown in Fig. 22. In the surrogate study, reagent-grade ZrO_2 (87.19 wt%), CaO (10.12 wt%), CeO_2 (2.69 wt%), stearic acid (1 wt%), and polyethylene glycol (1 wt%) were dry ball milled for 24 h, using ZrO_2 milling media. The milled powder was uniaxially pressed into pellets (6.5 mm x 6.0 mm) at a pressure of 310 MPa. The green pellets were then sintered for 5 h in an 80% N_2, 20% O_2 atmosphere at three temperatures (1200, 1400, and 1700°C). Pellet samples were cooled from the sintering temperature at an average rate of 10°C / min.

The flow diagram for the fabrication of NF fuel is shown in Fig. 23. Reagent-grade ZrO_2 (87.19 wt%) and CaO (10.12 wt%) were blended with weapons-grade PuO_2 (2.69 wt%) by dry ball milling for 4 h, using ZrO_2 milling media. Stearic acid (0.2 wt%) and polyethylene glycol (0.2 wt%) served as a lubricant and binder, respectively. The powder mixture was subsequently cycled six times through a high-energy vibratory mill containing ZrO_2 milling media. The milled powder was granulated and subsequently pressed into green pellets using a uniaxial hydraulic press. The green pellets were sintered for 6 h in a 94% argon, 6% hydrogen atmosphere at a temperature of 1700°C.

The flow diagram for the fabrication of EMOX fuel is shown in Fig. 24. Reagent-grade ZrO_2 (4.63 wt%) and CaO (0.462 wt%) were blended with weapons-grade PuO_2 (10.97 wt%) and depleted UO_2 (83.94 wt%) by dry ball milling for 4 h using tungsten

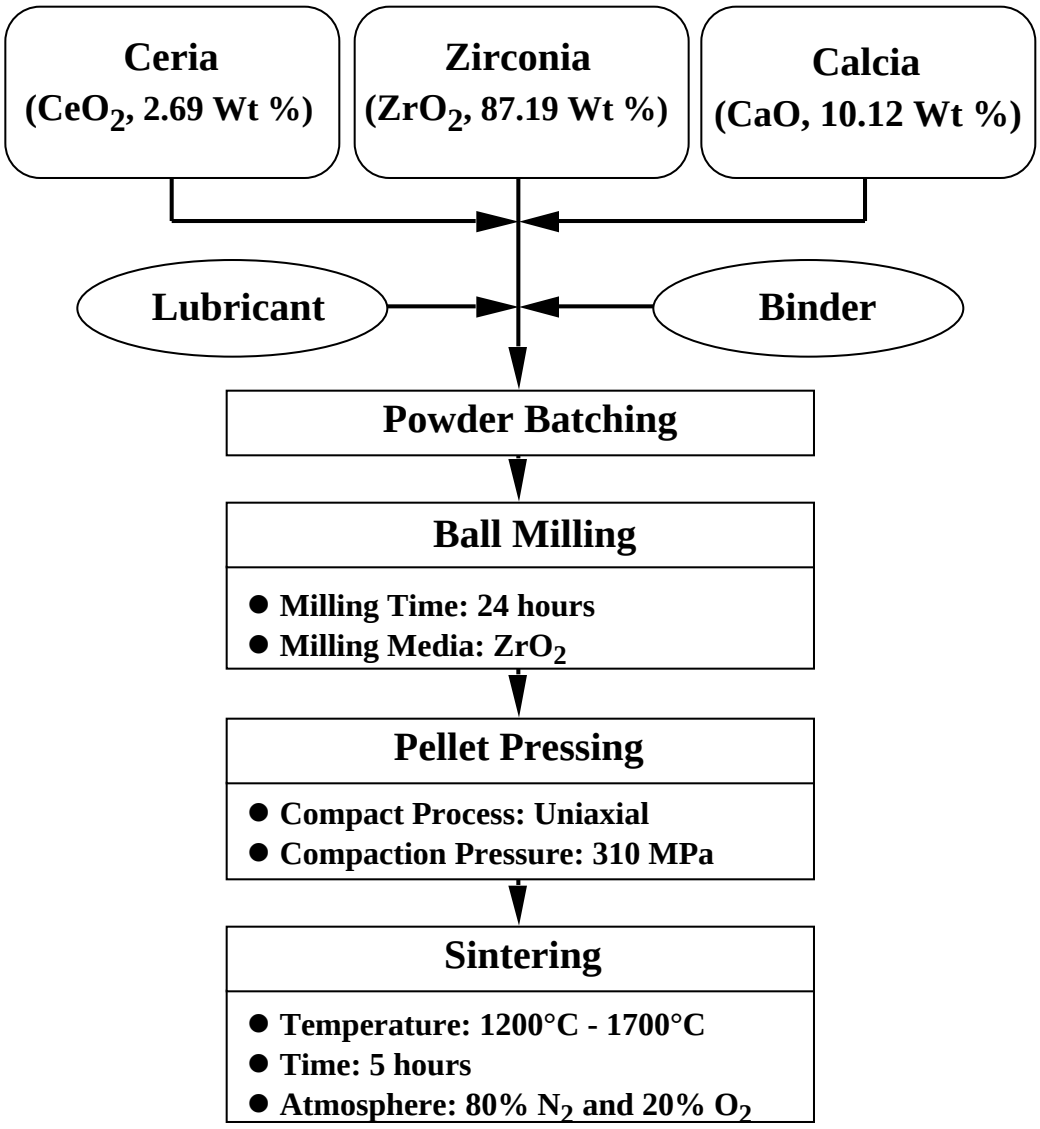

Fig. 22. Flow diagram for fabrication of surrogate NF fuel pellet.

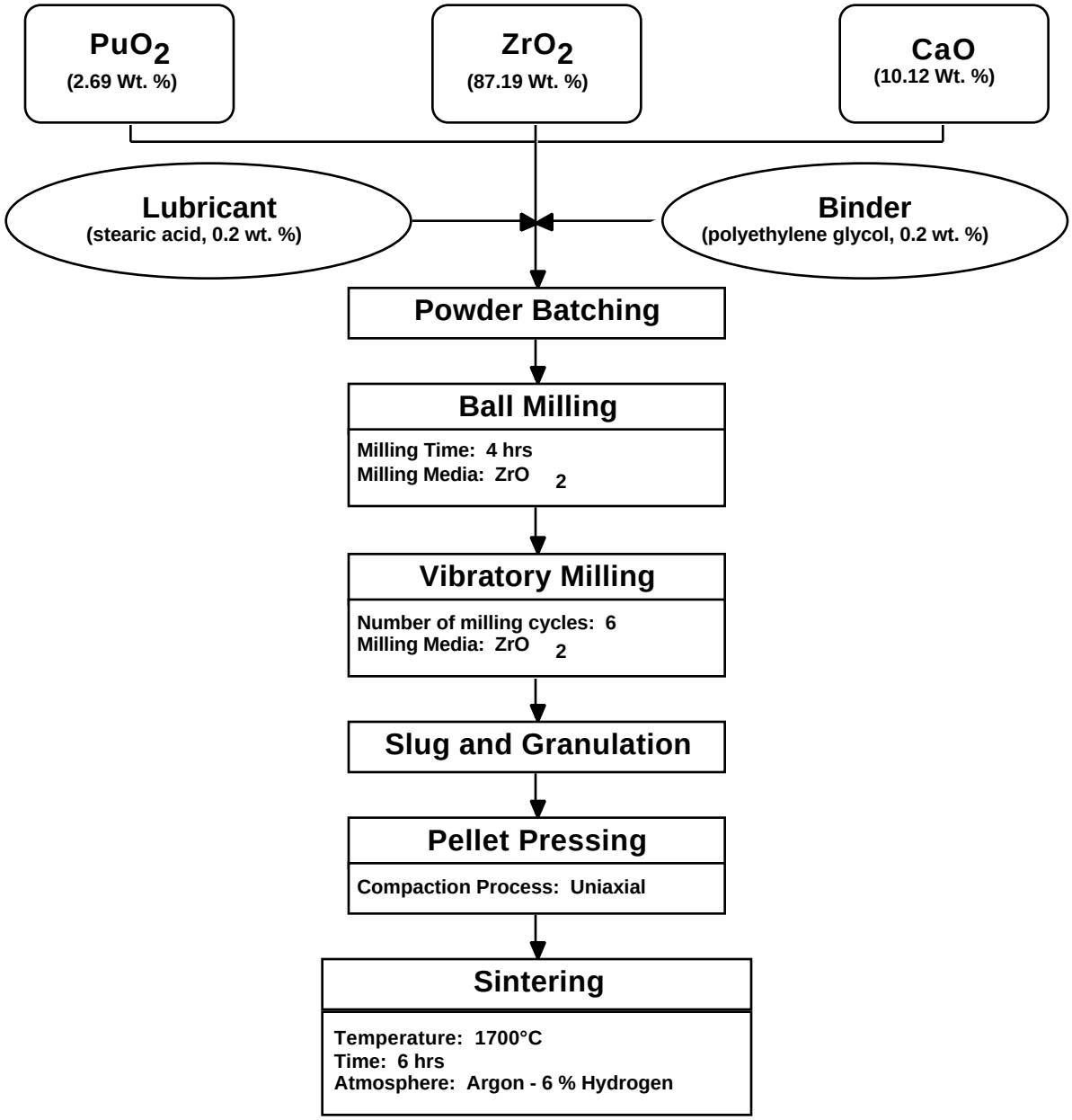

Fig. 23. Flow diagram for fabrication of NF fuel pellet.

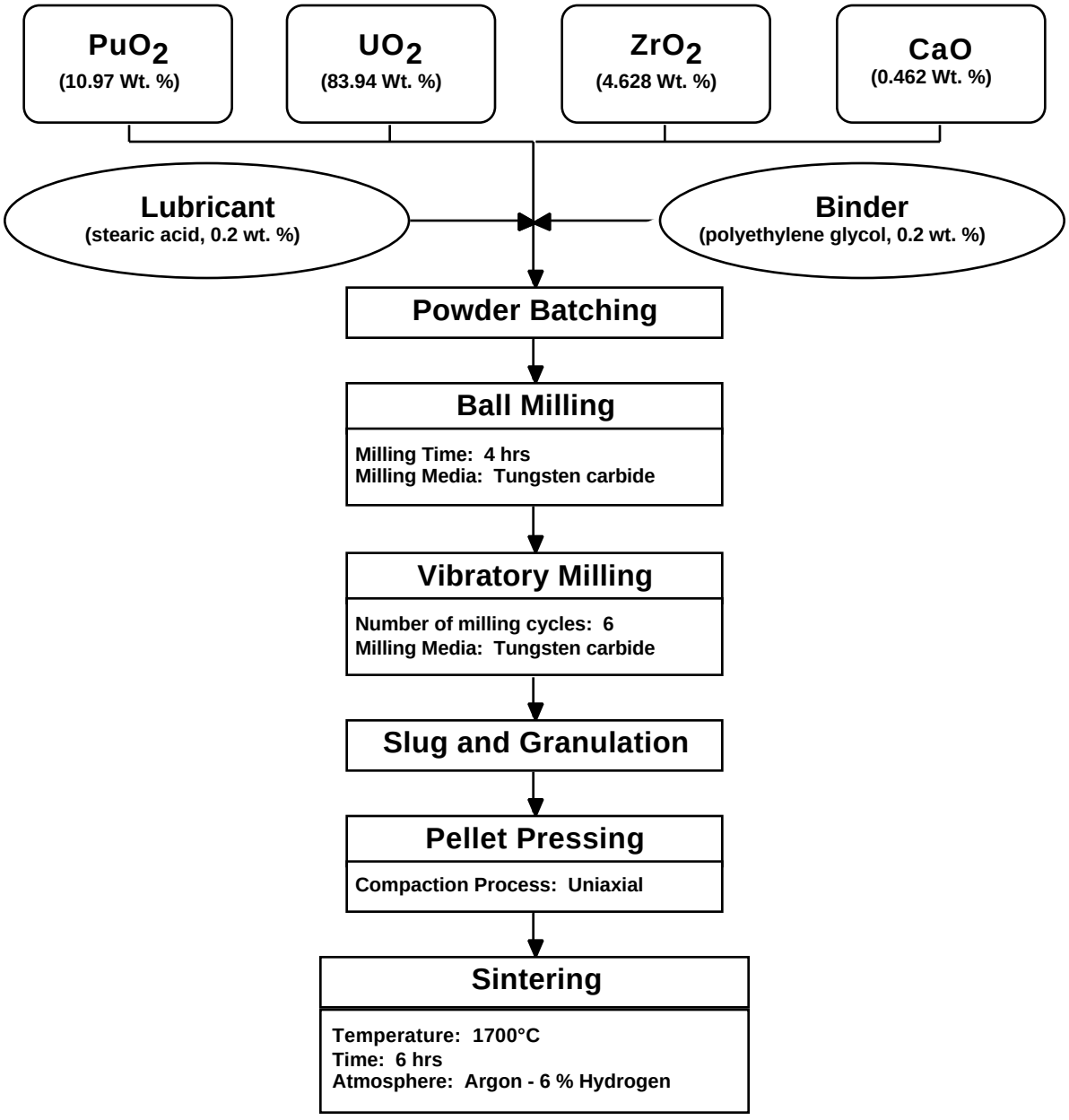

Fig. 24. Flow diagram for fabrication of EMOX fuel pellet.

carbide milling media. Stearic acid (0.2 wt%) and polyethylene glycol (0.2 wt%) served as a lubricant and binder, respectively. The powder mixture was subsequently cycled six times through a high-energy vibratory mill containing tungsten carbide milling media. The milled powder was granulated and subsequently pressed into green pellets using a uniaxial hydraulic press. The green pellets were sintered for 6 h in a 94% argon, 6% hydrogen atmosphere at a temperature of 1700°C.

Fuel Pellet Characterization

Sintered pellets were ground in an agate mortar and subsequently analyzed for crystalline phase content using x-ray diffractometry (XRD). The bulk density and volume percent of open and closed porosity were determined using the Archimedes method in bromobenzene. Grain and pore structure including average grain size and grain size distribution were determined using optical microscopy (OM) and SEM analysis. Chemical homogeneity was evaluated using electron microprobe analysis.

XRF Sample Preparation and Analysis

As shown in Fig. 25, the sample was prepared by mixing one gram of the analyte powder with five grams of stearic acid powder. The powders were blended in a SPEX mixer/mill for 5 min. The powder mixture was subsequently pressed into an aluminum cup (31 mm x 5 mm) using a 10-ton applied force. The cup containing the compressed powder was placed in a 40-mm plastic cell and sealed with a 4-mm Mylar sheet. The sealed cell was subsequently placed in a specimen cup with an additional sheet of Mylar film.

A Siemens SRS 300 wavelength dispersive XRF spectrometer equipped with a rhodium x-ray tube and helium purge system was used to detect the presence of zirconium, cacium, uranium, plutonium, cerium, and gallium in the surrogate, NF, and EMOX fuels. For the analysis, the specimen cup was placed directly into the sample port of the spectrometer. A collimator served to reduce the radiation burden on the detectors. Only analyte x-rays and a small portion of radiation impinged on the detector system.

RESULTS AND DISCUSSION

Surrogate Nonfertile Fuel Fabrication

The quality of the precursor and process blend powder will determine the characteristics of the final sintered fuel pellet. Therefore, a complete characterization of these powders was made to give confidence to the end results. Scanning electron micrographs of the ZrO_2, CaO and CeO_2 precursor powders are shown in Figs. 26, 27, and 28, respectively. The ZrO_2 powder consisted of granules formed by the spray drying method. The granules ranged in size from ~25 mm to

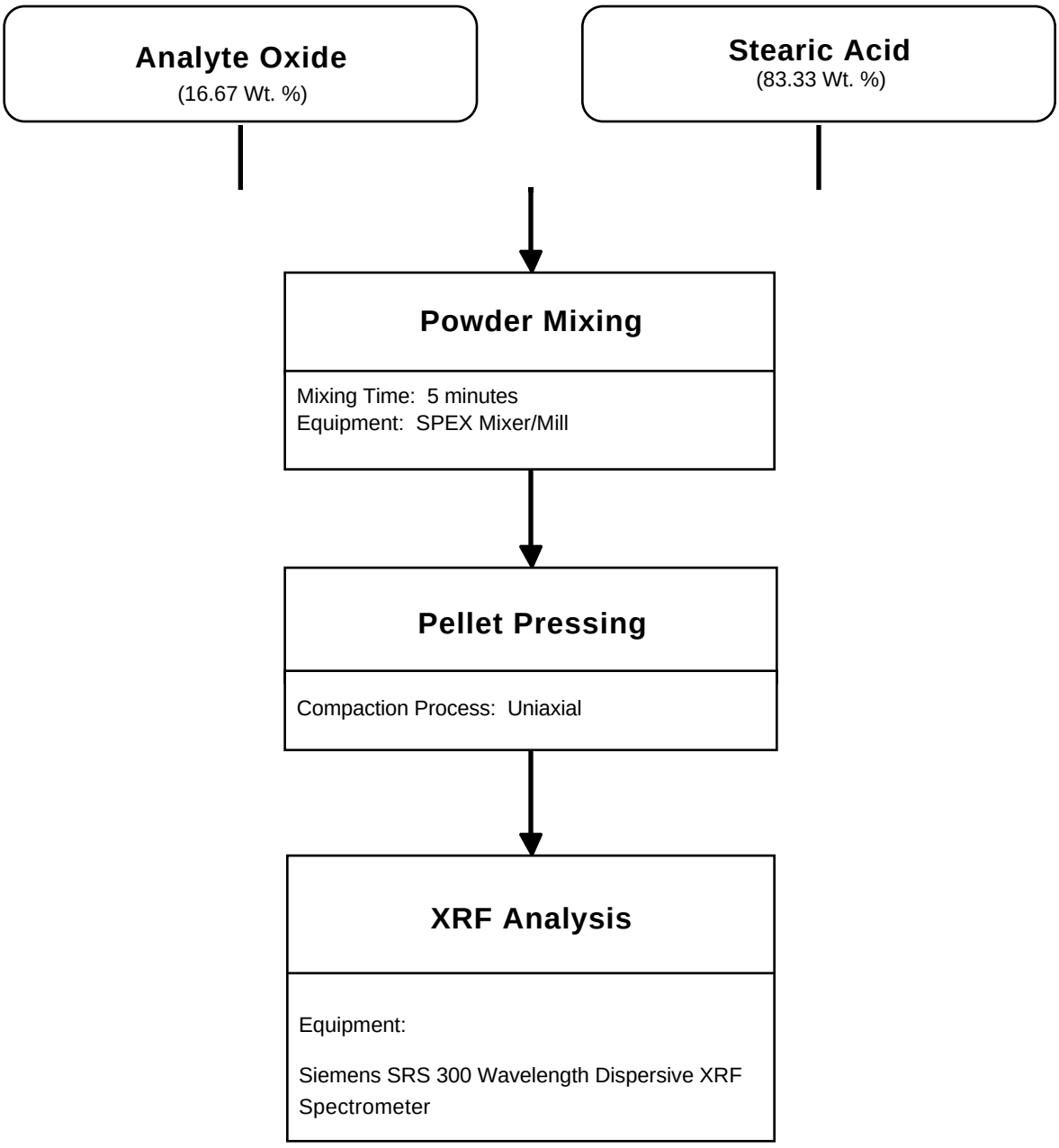

Fig. 25. Flow diagram for fabrication and testing of XRF sample.

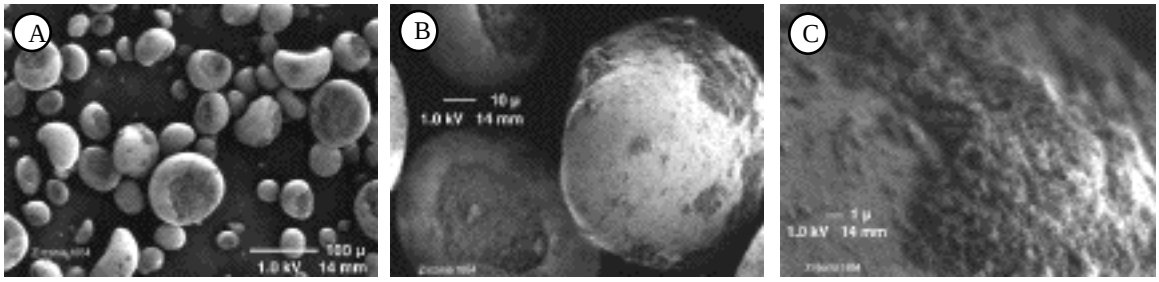

Fig. 26. Scanning electron micrographs of ZrO_2 powder: (A,B) granules formed by the spray drying method, and (C) surface of a granule.

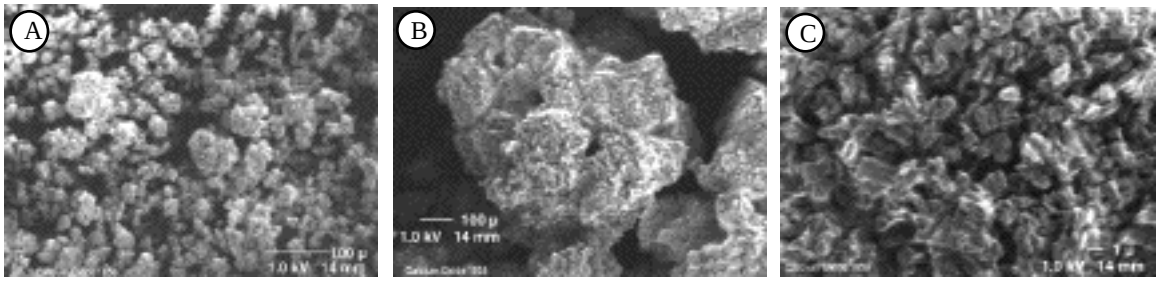

Fig. 27. Scanning electron micrograph of CaO powder: (A,B) particle aggregates, and (C) surface of aggregate.

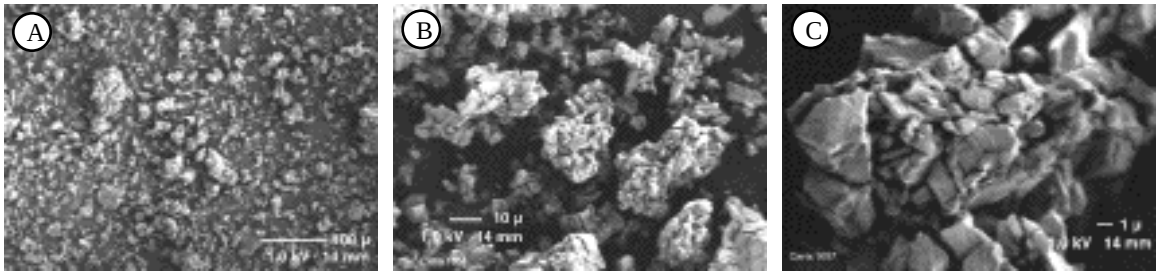

Fig. 28. Scanning electron micrograph of CeO_2 powder: (A,B,C) particle aggregates.

~100 mm. Submicron particles of zirconia are visible on the surface of the individual granules. The CaO powder consisted of aggregates ranging in sizes from ~25 to ~100 mm. The CeO_2 powder consisted of aggregates ranging in size from ~25 to ~75 mm. Individual CeO_2 grains ranging in size from 3 to 5 mm are visible within the aggregates. The particle size and specific surface area measurements of the precursor powders are shown in Table II.

As shown in Fig. 29, large (>500 mm) agglomerates were formed as a result of the ball milling of the precursor powders. The scanning electron micrographs show a broad particle size distribution. Submicron particles are visible on the surface of the agglomerates. The equivalent spherical diameter of the ball milled powder was determined to be 87.3 mm.

TABLE II
PARTICLE SIZE AND SPECIFIC SURFACE AREA MEASUREMENTS FOR SURROGATE NONFERTILE FUEL

Precursor Powder	Equivalent Spherical Diameter (μm)	Specific Surface Area (m^2/g)
ZrO_2	16.4	13.81
CaO	32.3	1.72
CeO_2	21.7	4.92

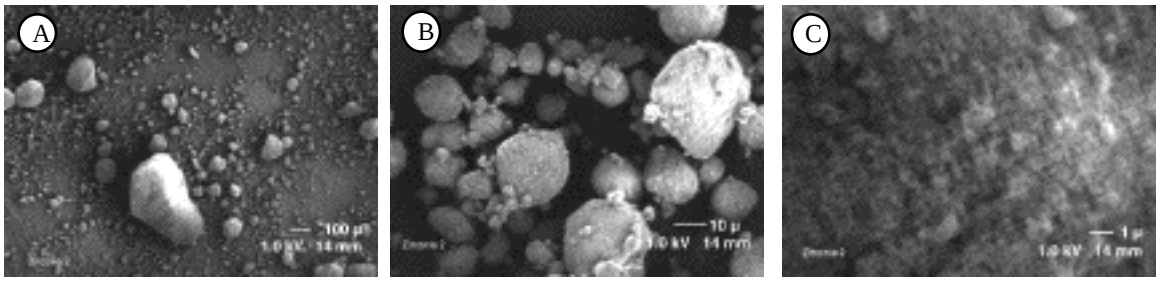

Fig. 29. Scanning electron micrograph of ball milled powder: (A,B) particle agglomerates, and
(C) surface of agglomerates.

As shown in Fig. 30, a significant increase in the bulk density of the surrogate fuel pellet occurred between the sintering temperatures of 1200 and 1400°C. This increase in density from 2.94 to 4.24 g/cm^3 corresponds to a decrease in open porosity (vol%) from 47.3% to 20.3%. An additional increase in bulk density occurred between the sintering temperatures of 1400 and 1700°C. This increase in density from 4.24 to 4.67 g/cm^3 corresponds to a significant decrease in open porosity (vol%) from 20.3 to 0.281%. The 4.67 g/cm^3 sintered density corresponds to a sintered density of 88.5% of theoretical.

The densification data shown in Fig. 30 indicate that dry ball milling of the precursor powders did not produce a highly reactive powder for sintering. The poor densification (<95% theoretical density) can be attributed to the powder agglomeration that resulted from ball milling the mixture of precursor powders for 24 h. Also, the particle morphology of CaO is not characteristic of highly reactive powders. Specifically, as shown in Table II, the particle size of CaO is significantly larger than the particle size of ZrO_2. Highly reactive powders typically have a particle size of 1 μm or less. Also, the specific surface area of CaO is significantly less than the specific surface area of ZrO_2.

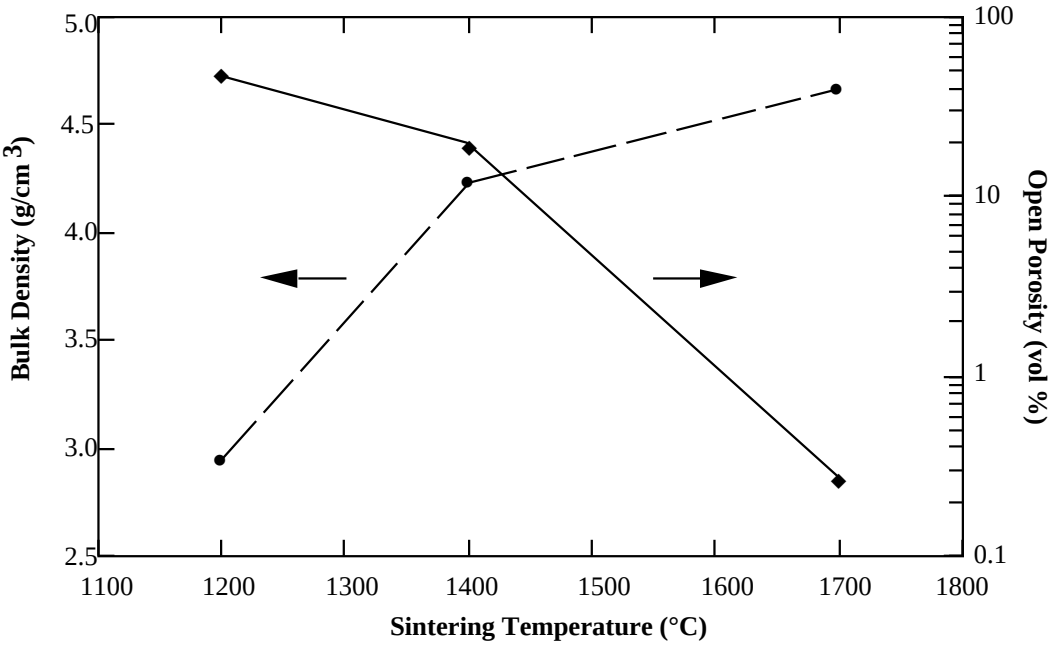

Fig. 30. Densification behavior of surrogate NF fuel pellets.

Figure 31 shows the x-ray powder diffraction pattern of the surrogate fuel sintered at 1200, 1400, and 1700°C. The cubic crystalline phase, $Ca_{0.15}\ Zr_{0.85}\ O_{1.85}$ is present in the surrogate fuel sintered at 1200, 1400, and 1700°C. This cubic phase is the calcia-stabilized form of zirconia corresponding to a CaO content of approximately 20 mole%. The orthorhombic crystalline phase, $CaZrO_3$, is present in the surrogate fuel sintered at 1200 and 1400°C. The CeO_2 precursor is present in the surrogate fuel sintered at 1200 and 1400°C. For a sintering time of 5 h, the XRD data indicate that a sintering temperature of between 1400 and 1700°C is required to form a solid solution of CeO_2 in calcia-stabilized zirconia.

Figure 32 shows the development of the surrogate fuel pellet microstructure as a function of sintering temperature. The dark areas in the optical micrographs indicate the presence of pores (intergranular and intragranular) within the sintered pellet. The pellet porosity decreased with an increase in sintering temperature from 1400 to 1700°C. In addition to densification, grain growth occurred as a result of increasing the sintering temperature from 1400 to 1700°C. As shown in Fig. 32, the average grain size for the pellet sintered at 1400 and 1700°C was 8 and 20 mm, respectively.

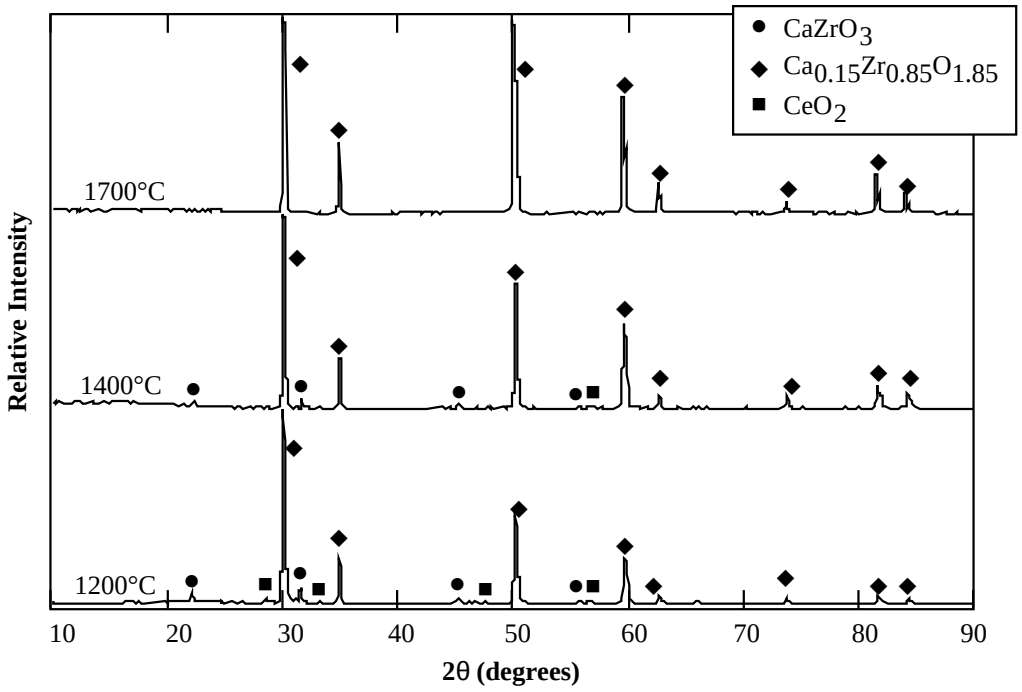

Fig. 31. X-ray diffraction pattern of sintered surrogate NF fuel pellet.

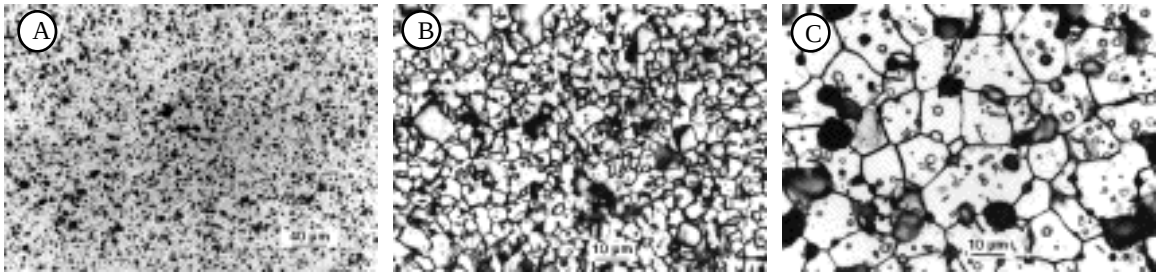

Fig. 32. Optical micrograph of surrogate NF fuel pellet sintered at (a) 1700, (b) 1400, and (c) 1700°C.

Electron microprobe analysis detected chemical inhomogeneity in the sintered surrogate fuel pellet. As shown in Fig. 33, a quantitative radial scan across the pellet at 200 µm steps detected a region of low zirconium and high calcium content. Table III lists the average concentrations for oxygen, calcium, zirconium, cerium, and hafnium for the matrix and nonhomogeneous regions. As shown in Table III, a minor phase with a relatively high concentration of calcium was detected near one edge of the pellet. The electron microprobe radial scan indicates that ball milling of the precursor powders did not homogenize the precursor powders.

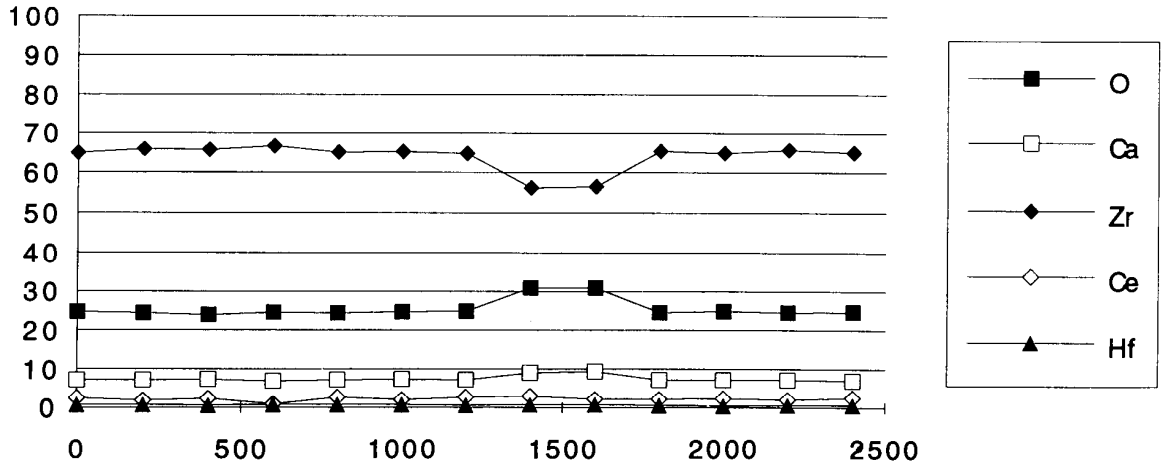

Fig. 33. Electron microprobe radial scan of surrogate NF fuel pellet.

TABLE III
ELECTRON MICROPROBE ANALYSIS OF SINTERED SURROGATE NONFERTILE FUEL PELLET

Pellet Region	Wt%				
	O	Ca	Zr	Ce	Hf
Matrix	24.6	7.17	65.41	2.16	0.64
1200–1800 μm	30.92	9.25	56.46	2.55	0.82
Pellet edge	24.9	22.4	51.7	0.58	0.51

NF Fuel Fabrication

Nonfertile fuel containing weapons-grade plutonium was fabricated using the solid-state reaction method. Figure 34 shows the particle morphology of the PuO_2 powder. Table IV lists the particle size and surface area data for the precursor powders. Vibratory milling of the precursor powders produced a powder with a specific surface area equal to 20.98 m^2/g. Green pellets were pressed to a 56.8% theoretical density. The typical green pellet had a diameter of 9.27 mm and a length of 10.16 mm. The green pellets were sintered to a density of 4.77 g/cm^3. The nonfertile fuel corresponds to 89.7% of theoretical sintered density.

The volume percent of open porosity for the sintered pellet was 1.44%, and the volume percent of closed porosity was determined to be 8.98%.

The additional fabrication step of vibratory milling proved beneficial for producing a more reactive precursor powder for sintering. Specifically, an increase from 88.5% of theoretical sintered density for the surrogate fuel to 89.7% of theoretical density for NF fuel indicated that comminution by vibratory milling produced a more

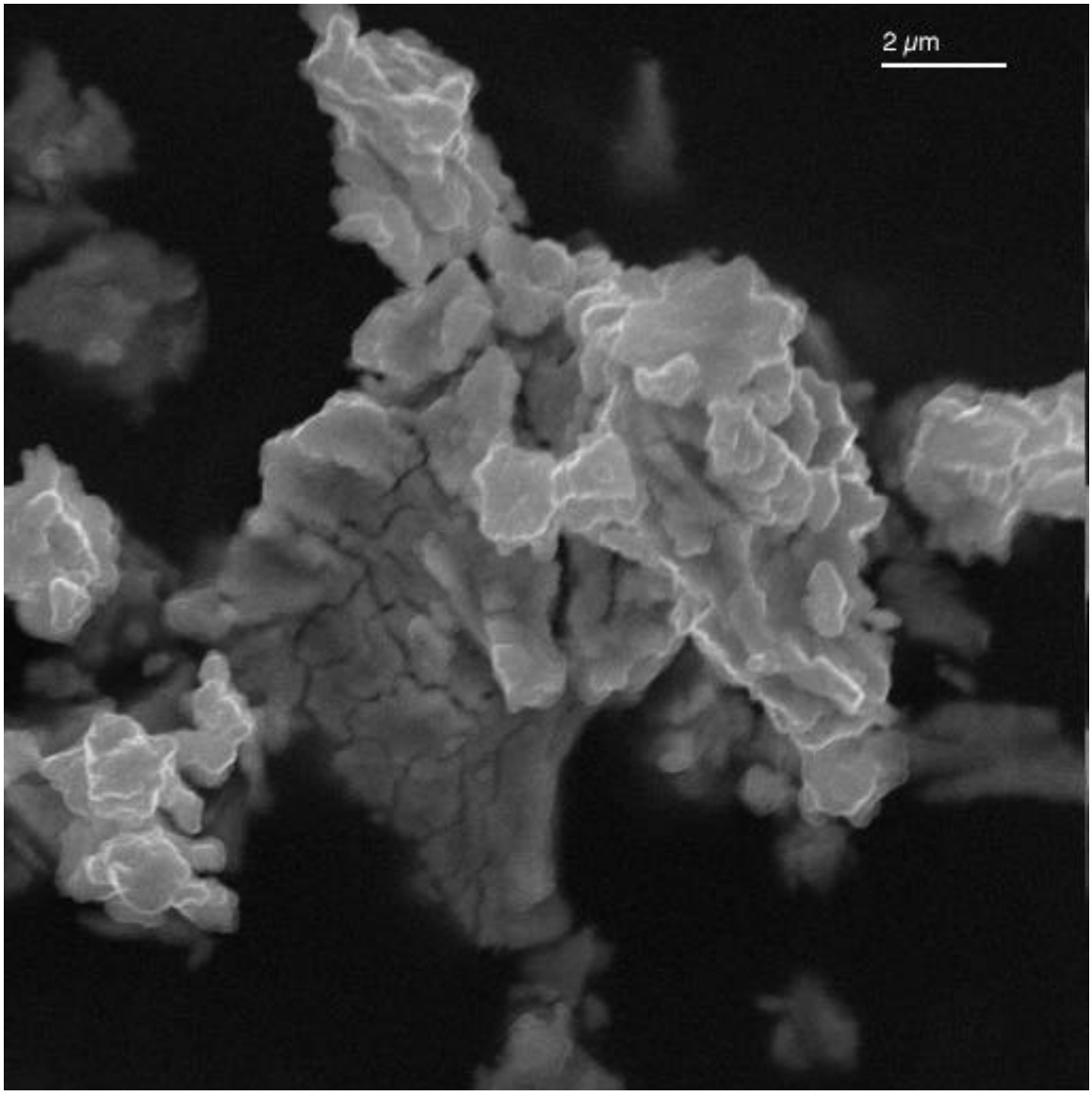

Fig. 34. Scanning electron micrograph of weapons-grade $Pu0_2$ powder.

TABLE IV
PARTICLE SIZE AND SPECIFIC SURFACE AREA MEASUREMENTS FOR NON-FERTILE FUEL

Precursor Powder	Equivalent Spherical Diameter (μm)	Specific Surface Area (m^2/g)
ZrO_2	1.95	23.99
CaO	32.3	1.72
PuO_2	14.6	5.52

reactive precursor powder. However, as shown in Fig. 35, porosity is clearly present in the sintered fuel pellet. The dark areas in the optical micrograph indicate the presence of intergranular and intragranular pores within the microstructure. As shown in Fig. 35, significant grain growth occurred as a result of sintering the green pellets for 6 h at 1700°C. Grain sizes range from 10 to >50 µm.

EMOX Fuel Fabrication

EMOX fuel containing weapons-grade plutonium was fabricated using the solid-state reaction method. Figure 36 shows a typical sintered pellet of EMOX fuel. Table V lists the particle size and surface area data for the precursor powders. Vibratory milling of the precursor powders produced a powder with a specific surface area equal to 4.12 m^2/g. Green pellets were pressed to 58.8% of theoretical density. The typical green pellet had a diameter of 9.27 mm and a length of 10.22 mm. The green pellets were sintered to a density of 10.12 g/cm^3. The sintered density of the EMOX fuel corresponds to 96.8% of theoretical. The volume percent of open porosity for the sintered pellet was 0.164%, and the volume percent of closed porosity was determined to be 3.04%. The typical microstructure of the sintered EMOX fuel pellet is shown in Figs. 37 and 38. The dark areas in the optical micrograph indicate the presence of pores within the microstructure. As shown in Fig. 38, the grain size is approximately 10 µm.

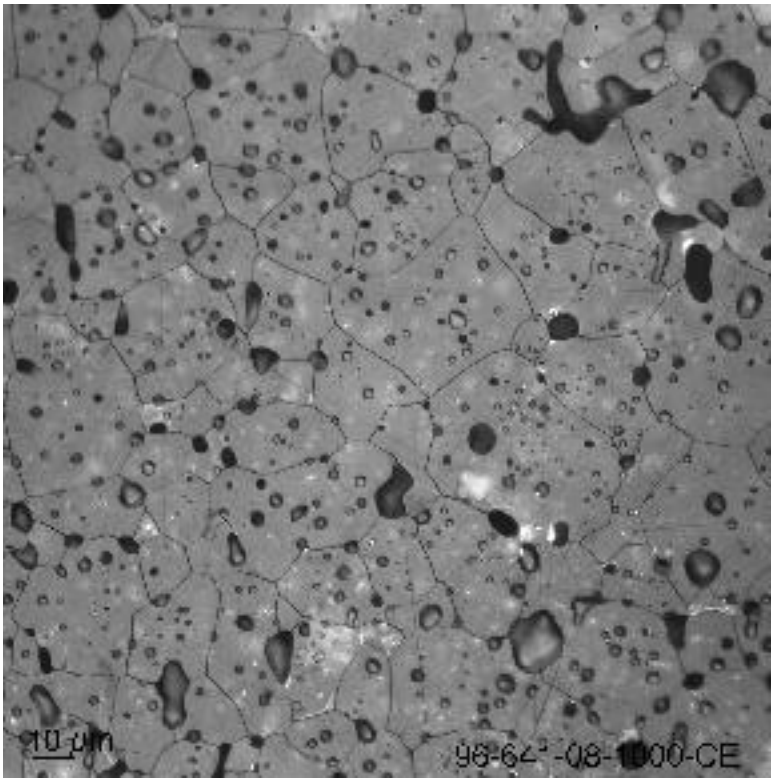

Fig. 35. Optical micrograph of NF fuel (Magnification: 1000x).

Fig. 36. Sintered EMOX fuel pellet.

TABLE V
PARTICLE SIZE AND SPECIFIC SURFACE AREA MEASUREMENTS FOR EMOX FUEL

Precursor Powder	Equivalent Spherical Diameter (μm)	Specific Surface Area (m^2/g)
UO_2	3.00	2.78
ZrO_2	2.45	3.32
CaO	32.3	1.72
PuO_2	14.6	5.52

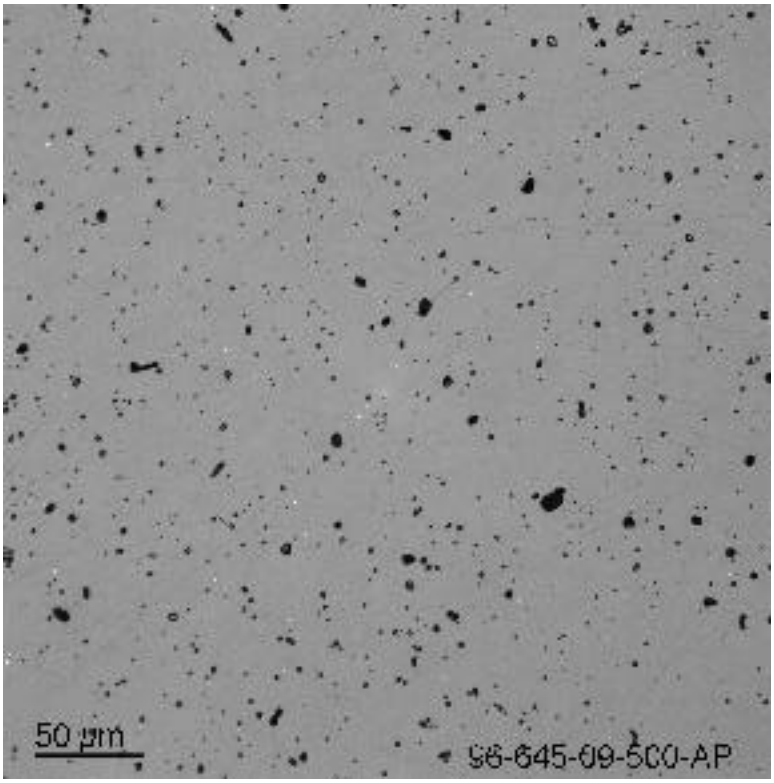

Fig. 37. Optical micrograph of EMOX fuel (magnification: 500x).

XRF Analysis

XRF spectrometry proved useful for detecting zirconium, calcium, cerium, plutonium, uranium, and hafnium in the precursor powders. Specifically, the XRF scan shown in Fig. 39 indicates that 0.5 wt% of CaO in the fuel can be detected using XRF analysis. This concentration corresponds to approximately 800 ppm of CaO in the sample pellet and subsequently less for the analyte calcium. The XRF scan shown in Fig. 40 indicates that 2.69 wt% of PuO_2 in the NF fuel can be detected using XRF analysis. The XRF scan shown in Fig. 41 indicates that 0.5 wt% of gallium in the weapons-grade plutonium can be detected. This concentration corresponds to approximately 800 ppm of gallium in the sample pellet.

SUMMARY AND CONCLUSIONS

NF and EMOX fuels have been fabricated using the solid-state reaction method. Precursor powders were successfully blended and milled using a combination of ball milling and high-energy vibratory milling. Sintering data for EMOX fuel indicated that significant densification occurred at a temperature of 1700°C. However, the presence of CaO in surrogate and NF fuels and excessive ball milling of the surrogate fuel inhibited densification of the fuel pellet. Comminution of the CaO precursor powder will be required to obtain a high-density NF fuel.

Fig. 38. Optical micrograph of EMOX fuel (magnification: 1000x).

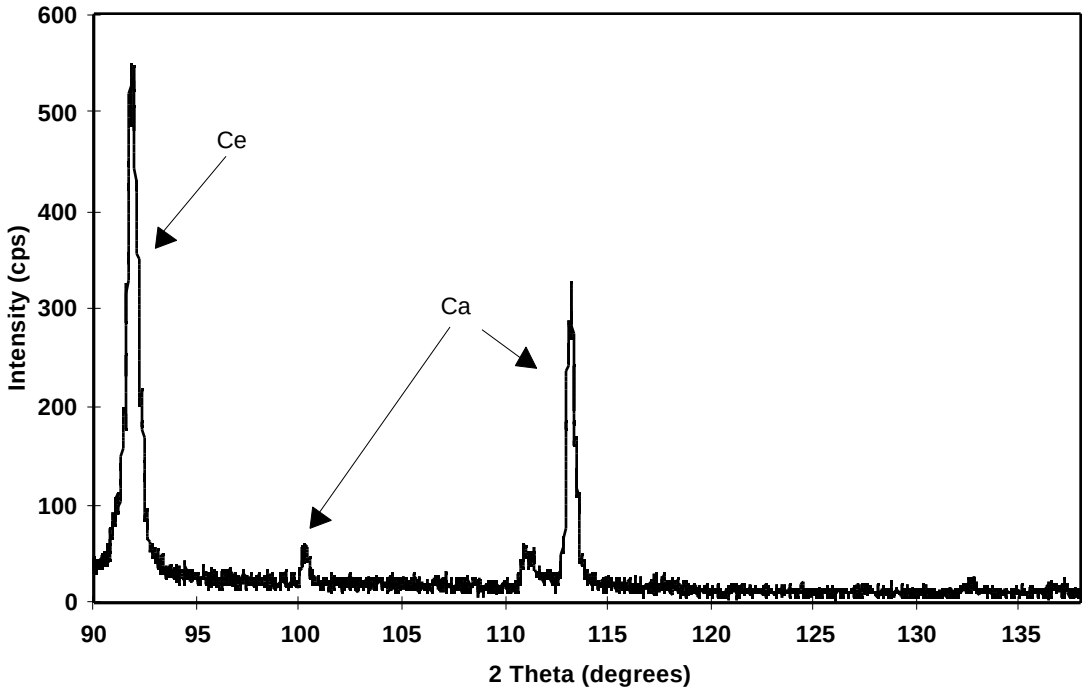

Fig. 39. XRF wavelength dispersive scan of surrogate NF fuel.

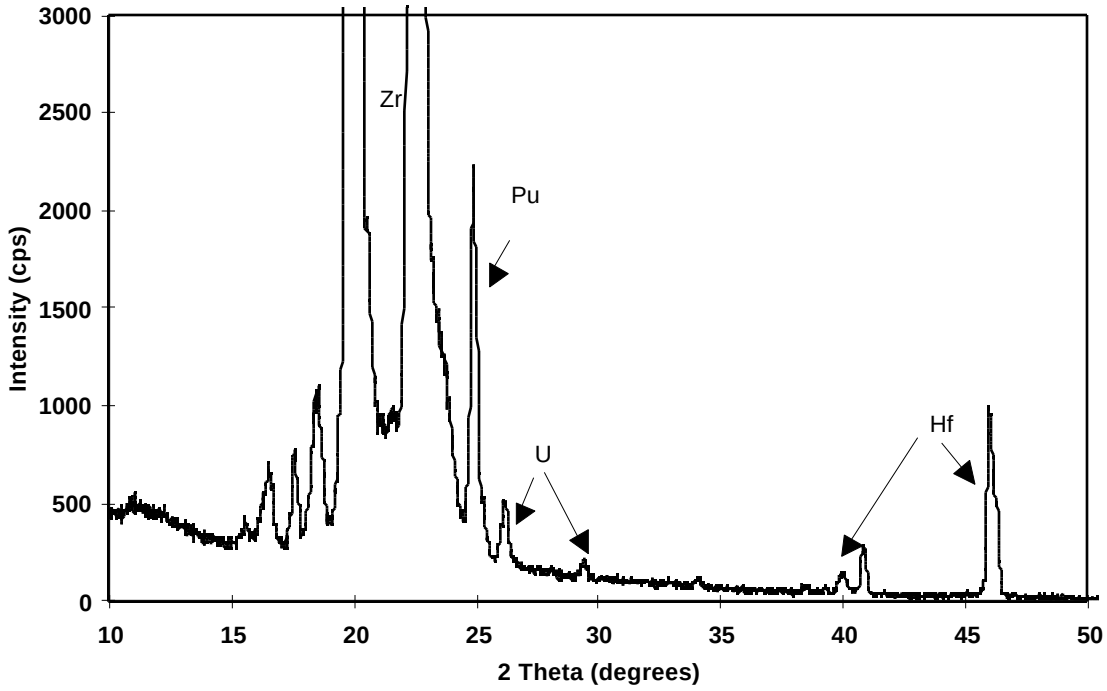

Fig. 40. XRF wavelength dispersive scan of NF fuel.

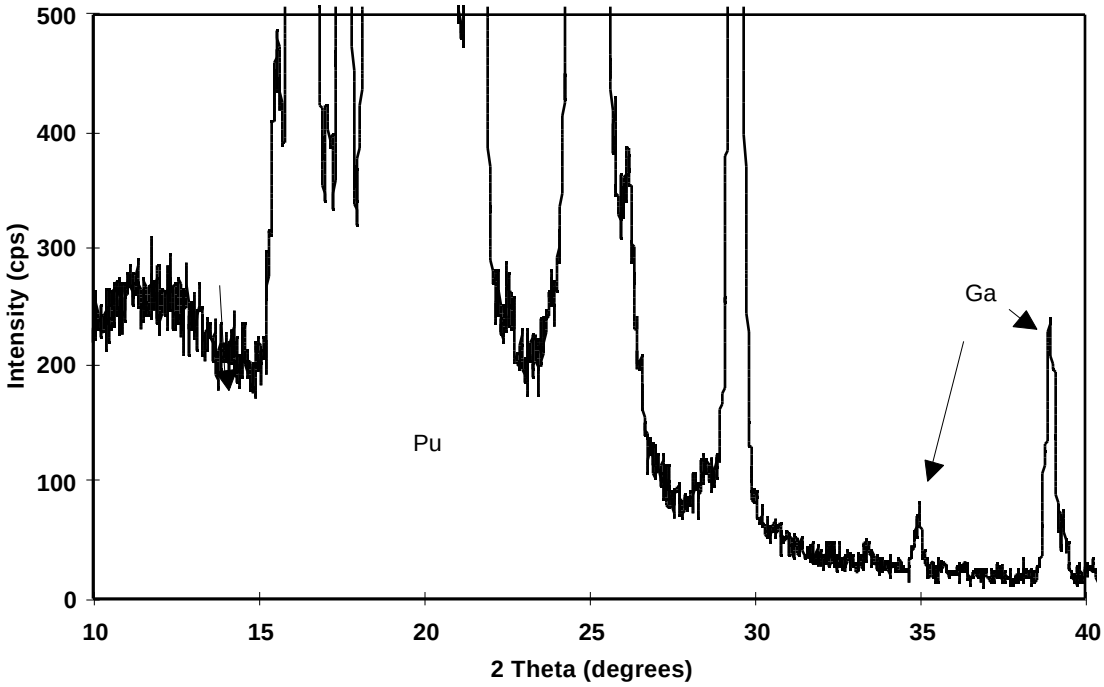

Fig. 41. XRF wavelength dispersive scan of PuO_2 powder.

FUTURE OBJECTIVES

Additional EMOX and NF fuel compositions will be fabricated using depleted UO_2, weapons-grade PuO_2, Er_2O_3, and Y_2O_3. Specifically, the feasibility of fabricating EMOX compositions with NF wt% fractions of 17.0, 32.5, and 65.5 will be determined. The feasibility of fabricating NF fuel using yttria-stabilized zirconia and Er_2O_3 as a depletable neutron absorber will be investigated. X-ray diffraction spectrometry will be used to determine the extent of solid solution formation in the EMOX and NF fuels. Using such techniques as x-ray diffraction spectrometry, ceramography, transmission electron microscopy, and electron probe analysis, preliminary phase diagrams for the oxide systems PuO_2-ZrO_2-CaO-Er_2O_3 and UO_2-PuO_2-ZrO_2-CaO will be determined.

X-ray fluorescence spectrometry will be further developed to analyze concentrations of zirconium, calcium, yttrium, plutonium, uranium, erbium, and gallium in precursor powders and sintered pellets of EMOX and NF fuel compositions. Analytical standards will be prepared to develop quantitative XRF spectrometry.

CONCLUSIONS

Initial analyses have shown that the EMOX concept can be an attractive plutonium management tool. Small additions of the inert material to standard MOX fuel increase the overall plutonium destruction within the system, and the composition can be tailored to suit a particular management strategy, including zero net plutonium production or high plutonium destruction options. Initial compositions can be designed as slight perturbations from standard MOX fuel for ease in licensability and then modified accordingly to provide a smooth transition to implementation of higher plutonium destruction nonfertile fuels.

Initial fabrication experiments indicate the possibility of producing EMOX and NF fuels using standard fabrication processes (cold press and sinter). More data are required, however, to determine the appropriate process parameters, especially with regard to fuel types that contain a large fraction of the nonfertile component.

Future work includes the development of global models to quantify the benefits of employing EMOX and NF fuels in commercial power reactors. In addition, more detailed physics and thermal-hydraulic models are being created in an effort to better test the expected in-reactor performance of the fuel. At the appropriate time, experiments will be initiated to demonstrate that the fuel performance is as predicted.

Fabrication experiments will continue investigating how changes in composition of the EMOX and NF fuels affect the required fabrication process parameters. Continued development of analytical techniques is also being pursued to better characterize the experimental results.

REFERENCES

1. National Academy of Sciences, Committee on International Security and Arms Control, "Management and Disposition of Excess Weapons Plutonium" (National Academy Press, Washington, DC, 1994).

2. Juan J. Casal, Rudi J. J. Stamm'ler, Eduardo Villarino, and Aldo Ferri, "HELIOS: Geometric Capabilities of a New Fuel Assembly Program," *Proceedings of the International Topical Meeting on Advances in Mathematics, Computations, and Reactor Physics*, CONF-910414 (Pittsburgh, Pennsylvania, April 1991) **2**, pp. 10.2 1-1–10.2 1.13.

3. J. Duderstadt and L. Hamilton, *Nuclear Reactor Analysis* (John Wiley & Sons, New York, 1976).

4. W. Marshall, *Nuclear Power Technology, Volume 2: Fuel Cycle* (Clarendon Press, Oxford 1983).

5. C. S. Olsen, "Non-Fertile Fuels Development for Plutonium and High-Enriched Uranium Dispositioning in Water Cooled Reactors," Idaho National Engineering Laboratory document INEL-95/0038 (September 1994).

6. H.R. Warner, "Evaluation of Low Density Single-Phase Cubic ZrO_2+UO_2 Fuels Stabilized with CaO," WAPD-292, UC-25: Metals, Ceramics, and Materials, TID-4500 (46th Edition), Westinghouse Electric Corporation (January 1966).

7. R.M. Berman, "The Homogenization and Densification of ZrO_2+UO_2 Fuels Under Irradiation," WAPD-301, UC-25: Metals, Ceramics, and Materials, TID-4500 (46th Edition), Westinghouse Electric Corporation (January 1966).

8. B.F. Rubin, R.M. Berman, and M.L. Bleiberg, "The Irradiation Behavior of ZrO_2+UO_2 Fuels," WAPD-264, UC-25: Metals, Ceramics, and Materials, TID-4500 (17th Edition), Westinghouse Electric Corporation (October 1962).

9. A. Boltax et al., "Ternary Fuel Performance Data for the Special Water Reactor," WSR-84-252, Westinghouse Electric Corporation Advanced Energy Systems Division (December 1984).